# Influence of corrosion effects on the seismic capacity of existing RC bridges

Pietro CRESPI[(1)], Marco ZUCCA*[(2)], Marco VALENTE[(1)], Nicola LONGARINI[(1)]

*(1) Department of Architecture, Built Environment and Construction Engineering*
*Politecnico di Milano, Milano, Italy*
*(2) Department of Civil, Environmental Engineering and Architecture*
*University of Cagliari, Italy*
** Corresponding author. E-mail: marco.zucca@polimi.it*

## Abstract

Recent collapse events of existing reinforced concrete bridges have increased the attention on the mandatory and suitable maintenance of these strategic constructions. In fact, most of these failures were due to an inadequate scheduling of maintenance interventions. One of the main issues concerning the load-bearing capacity of existing reinforced concrete structures is related to the corrosion of steel reinforcement caused by the carbonation phenomenon. Such aspect should not be even more overlooked considering the strategic role of infrastructures like the bridges of the Italian motorway network, mainly built around the 1960's and widely used even right now. Consequently, reinforced concrete bridges require the execution of maintenance interventions in order to guarantee an adequate safety level under both serviceability conditions and exceptional loads, also considering that they were often designed without taking into account seismic actions.
This paper analyses the seismic performance of five existing reinforced concrete bridges under several corrosion scenarios of piers steel reinforcement caused by the carbonation phenomenon. In particular, three different corrosion levels (slight, moderate and high) are considered by analysing the evolution of the phenomenon effects for a lifetime of the structure equal to 75 years. The seismic vulnerability is then evaluated by defining appropriate risk indices expressed in terms of peak ground acceleration and corresponding return period. The risk indices are determined by performing modal pushover analyses on finite element models, considering the corrosion effects in terms of steel rebars cross section reduction. Some correlations between corrosion levels and risk indices are drawn.



**Keywords**: *existing RC bridges, steel corrosion, concrete carbonation, modal pushover analysis, seismic vulnerability.*

## 1. Introduction

The interest about the conservation of existing reinforced concrete (RC) bridges has increased a lot in the last decades both for their strategic role and for the tragic collapses occurred under traffic or seismic actions [1-5]. Moreover, the intensification of the environmental pollution led to an increase of corrosion phenomena afflicting RC structures and to a reduction of their load-bearing capacity, both in service conditions and under exceptional loads. Therefore, different concrete mix designs were studied for improving the concrete durability [6-10]. Nevertheless, the corrosion of steel reinforcement is very common [11-14] and it is one of the most important reasons of the safety level reduction of motorway bridges [15-18].

In existing RC bridges, the carbonation phenomenon typically interests all the structural members whereas chloride ions attack mainly regards deck structures for the use of de-icing salts. Given that the seismic capacity of bridge structures strongly depends on the capacity of piers, the present work is focused on the corrosion induced by concrete carbonation.

Furthermore, many of the Italian motorway bridges were designed and built between 1960's and 1970's. At that time, only limited horizontal loads were considered in design practice. Thus, the combination of age issues and actual seismic hazard entails the need of evaluating the seismic vulnerability, in order to guarantee an adequate safety level, and to implement appropriate maintenance interventions.

According to the recent design codes developments, several approaches have been proposed to detect collapse mechanisms of the RC structures subjected to seismic actions. In particular, non-linear techniques like the pushover analysis [19,20] have been increasingly used, even if this kind of approach is basically limited to structures characterized by a predominant translational vibration mode. A different approach is the non-linear time history analysis, in which the definition of the seismic inputs, the modelling of strength/stiffness degradation and the correct interpretation of the damping evolution require great attention [21,22]. For these reasons and for the high computational cost, the non-linear time history analysis is not commonly used by designers.

Several researchers have proposed the use of fragility curves for the evaluation of the seismic vulnerability of existing RC bridges [23-25]. A further approach, developed in recent years, is the incremental dynamic analysis (IDA) technique [26,27].

In [28,29] the use of modal pushover analysis (MPA), a method initially proposed for the evaluation of the seismic response of unsymmetrical-plan buildings [30,31], is extended to the evaluation of the seismic behaviour of existing RC bridges. This method represents a development of the Response Spectrum Analysis (RSA) applied to the evaluation of the dynamic response of irregular structures, where a predominant vibration mode with high mass participation is not present and the contribution of higher vibration modes cannot be neglected. For these reasons, MPA seems particularly suitable for the analysis of the seismic response of existing RC bridges, often characterized by a complex dynamic behaviour involving several vibration mode shapes, particularly for the case of long-span and multi-span bridges with cantilever or frame piers. Given that the corrosion of steel reinforcement reduces the stiffness and strength of piers, corrosion effects should be taken into account in the analysis.

In this paper, the correlation between the corrosion level and the seismic performance of existing RC bridges is investigated through the variation of the risk indices of the structure, expressed in terms of peak ground acceleration (PGA) and corresponding return period ($T_R$), obtained considering two different types of pier collapse mechanisms: (i) the ductile mechanism and (ii) the brittle mechanism. At the same time, three corrosion levels (slight, moderate and high) are considered for different ages of the structure. The values of the risk indices are calculated through the procedure proposed in [32] where modal-pushover analyses are carried out through the implementation of simplified 3D finite element models (FEMs): bridges are modelled with beam elements and the non-linear behaviour of the structure is taken into account by proper plastic hinges located at the base of the piers (to limit the computational effort).

The proposed MPA procedure is applied on several existing RC bridges located in moderate to high seismicity areas of Northern Italy. Each model of the considered bridges is implemented through MIDAS Civil software [33]. Thus, by adopting the procedure described in [32], the evolution of the risk indices over time is investigated for five selected bridges, with reference to four different ages of the structures.

## 2. Structural Modelling and Analysis Method

As mentioned in Section 1, the analyses are performed by considering the approach described in [15,32] through the implementation of simplified FEMs where the piers, the pier caps and the decks are represented by beam elements, whereas the elastomeric bearings are introduced by elastic links having translational and rotational stiffness evaluated as reported in [34]. As shown in Fig. 1, the connection between the beam elements and the elastic links is guaranteed through a series of rigid links. The abutments are considered as perfect restraints applied to the base node of the elastic link modelling the elastomeric bearings on the top of the abutment (Fig. 2), whereas the foundations of the piers are modelled as fully constrained nodes at the base of each pier.

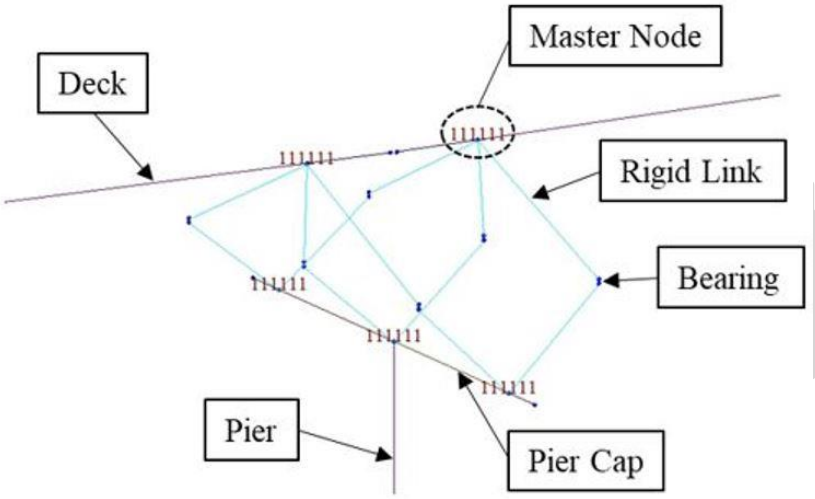


Figure 1. FEM implementation of the pier-deck connection.

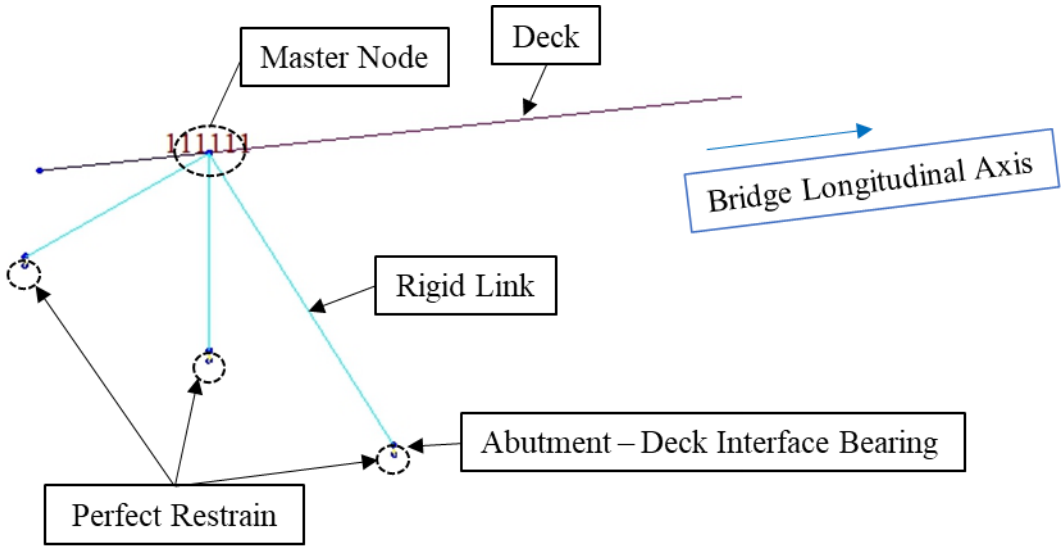


Figure 2. Abutment schematization.

The presence of non-structural elements, such as deck pavements and guard rails, is considered in the FEM through the application of distributed beam loads on deck beam elements, while deck cross beams are taken into account as concentrated nodal loads that are placed in correspondence with the position of cross beams along the deck longitudinal axis.
Once each structural element is implemented in the FEM, the reduction of the piers bending stiffness due to concrete cracking must be introduced to correctly evaluate the dynamic behaviour of the bridge. For this reason, specific scale factors, calculated through the moment-curvature ($M$-$\chi$) diagrams of the cross-section of the piers as reported in [35], are attributed to the concrete gross-section elastic stiffness of each pier. On the contrary, the deck stiffness is not scaled because it usually remains in the elastic field during the ground shaking [36,37]. In terms of masses, the FEM considers the sum of the structural and non-structural masses, whereas the traffic loads are not considered according to [38].
Two failure mechanisms are monitored for each pier: i) the ductile collapse mechanism, and (ii) the brittle collapse mechanism. The ductile collapse is related to the moment-curvature diagram of the cross-section of the pier, where an initial elastic branch is followed by a large strain hardening plastic behaviour. On the contrary, the brittle collapse mechanism is regulated by a linear load-displacement trend until reaching the ultimate shear resistance. The first collapse mechanism strictly depends on the rotational capacity of the plastic hinge, whereas the second one is directly controlled by the shear strength characterizing the considered structural element.
To model the non-linear behaviour of concrete, the Kent and Park model [39] is adopted, taking into account also the beneficial contribution on the concrete compressive strength provided by the confinement effect given by the stirrups, through the peak coefficient $K$, and the deterioration of the material in the softening phase, through the parameter $Z$. The Park Strain Hardening constitutive law [40] is used to model the behaviour of steel reinforcing bars (Fig. 3).
The non-linear behaviour of the bridge is included in the FEM by means of the introduction of suitable plastic hinges, defined as reported in [41,42], located at the base of the piers, where the activation of the ductile collapse mechanism can be expected (Fig. 4).



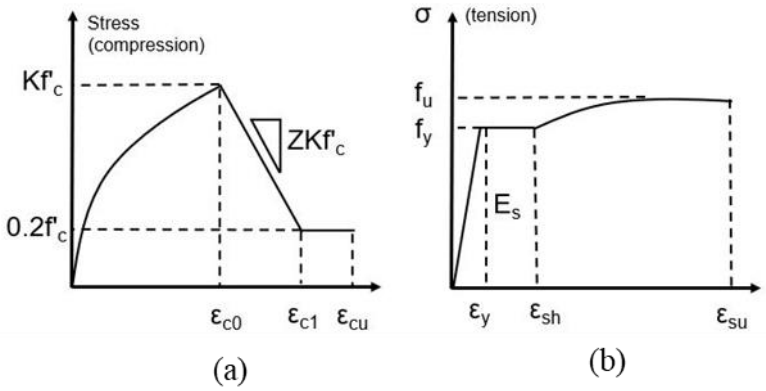


Figure 3. (a) Kent and Park and (b) Park Strain Hardening models.

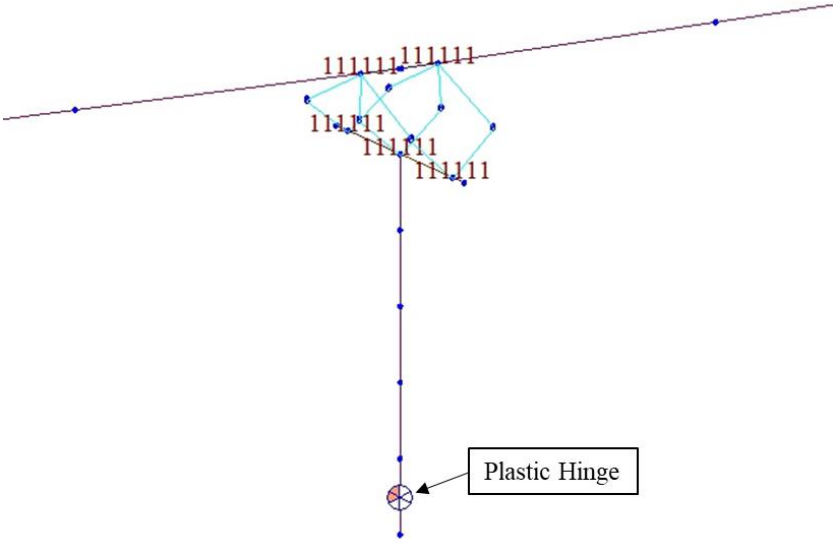


Figure 4. Position of the plastic hinge in the model.

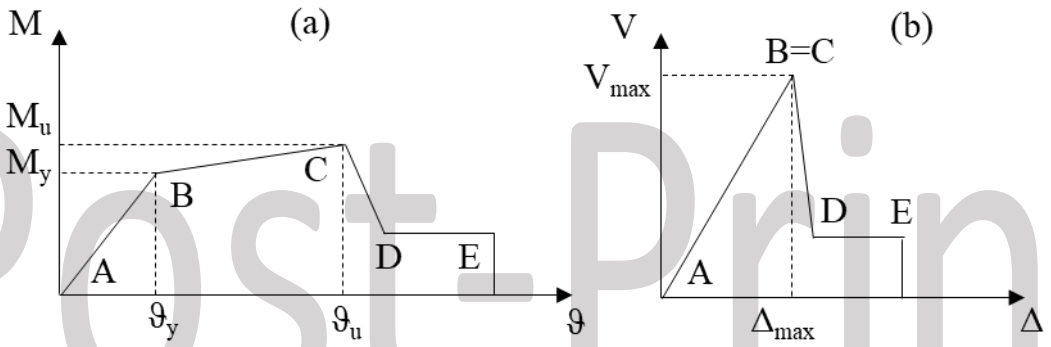




Figure 5. Definition of the collapse mechanisms: (a) ductile bending mechanism, and (b) brittle shear mechanism.

Two different verification criteria are considered in the following: the achievement of ¾ of the ultimate rotation $\vartheta_u$ (point C in Fig. 5a) is adopted to control the ductile failure mechanism, whereas, for the brittle collapse mechanism, the achievement of the maximum shear resistance ($V_{max}$, Fig. 5b) of the structural member is used. In this work, the cyclic shear resistance of piers is calculated, according to [43], with the following equation:

$$V_R = \frac{1}{\gamma_{el}}\frac{h-x}{2L_V}\min(N; 0.55A_c f_c) + \frac{1}{\gamma_{el}}(1 - 0.05min(5; \mu_\Delta^{pl})) \cdot \left[0.16max(0.5; 100\rho_{tot}) \cdot \left(1 - 0.16min\left(5; \frac{L_V}{h}\right)\right) \cdot \sqrt{f_c}A_c + V_w\right] \quad (1)$$

as a function of the sum of three terms depending on axial load, concrete strength, and transverse steel reinforcement of the pier. The safety factor $\gamma_{el}$ is equal to 1.15 for the primary seismic elements, $x$ is the neutral axis depth, $N$ is the axial load, $\mu_\Delta^{pl}$ is the ductility expressed in terms of rotation, $A_c$ is the cross-section area, $\rho_{tot}$ is the longitudinal ratio of steel reinforcement, $V_w$ is the shear resistance of the transverse steel reinforcement, and $L_v$ is the shear span.

The corrosion effects caused by concrete carbonation are introduced in the analyses through a simplified analytical model based on the progressive reduction of steel reinforcement diameter. As reported in Eq.(2), the penetration law in a generic concrete volume is characterized by a parabolic trend:

$$s = k \cdot t^{1/n} \tag{2}$$

where $s$ is the thickness of the carbonated layer of concrete, which increases as a function of the penetration rate coefficient $k$ with time $t$. For the existing RC bridges built around the 1960's, $n$ = 2 can be assumed because they were built with normal compacted concrete [44].
According to [45], in order to evaluate the residual service life $t_{res}$ of the structure, the initiation time $t_i$ and the propagation time $t_p$ are considered with the maximum expected rebar radius reduction $P_{lim}$ (evaluated according to the relevant limit state of the structure), as reported in Eq. (3):

$$t_{res} = t_i + t_p - t = \left(\frac{c}{k}\right)^2 + \frac{P_{lim}}{i_{corr}} - t \tag{3}$$

where $t$ is the age of the structure, $k$ is the penetration rate coefficient (expressed in mm/years$^{0.5}$), $i_{corr}$ is the mean corrosion current density (in μA/mm$^2$), and $c$ is the concrete cover thickness. As mentioned before, this work is focused on the seismic performance evaluation of existing RC bridges built around the 1960's. Given the design criteria adopted at the time, these bridges are not able to withstand the seismic actions foreseen by the current Italian design code [46]. For this reason, the evaluation of $t_{res}$ is not useful and the proposed approach directly considers the influence of the reduced area of steel rebars on the seismic performance of the bridges, according to the following Eqs. (4)-(5):

$$d(t) = d_0 - 2P(t) = d_0 - 2i_{corr}k(t - t_i) \tag{4}$$

$$A_s(t) = \pi[d_0 - 2i_{corr}k(t - t_i)]^2/4 \tag{5}$$



In particular, Eq. (4) is related to the variation of the steel rebar diameter $d$ as a function of the corroded thickness $P(t)$ and Eq. (5) is referred to the variation of the cross-section area $A_s$.
Considering three different corrosion levels (slight, moderate and high), the following values of $i_{corr}$ can be detected according to [47]: $i_{corr}$ = 0.1 μA/cm$^2$ for the slight corrosion level, $i_{corr}$ = 1 μA/cm$^2$ for the moderate corrosion level and $i_{corr}$ = 5 μA/cm$^2$ for the high corrosion level.
The reduction of the steel reinforcement diameter is calculated by the difference between the initial steel rebar diameter $d_0$ and the actual one $d(t)$. The reduction is again related to the initiation time $t_i$ (considered as a statistical variable) and the corrosion current density $i_{corr}$ (determined from experimental results or design codes). Therefore, starting from a cover thickness value equal to 25 mm, the procedure was repeated considering different types of concrete.
In this work, the following parameters have been chosen: (i) water/cement ratio $w/c$ = 0.6 and initiation time $t_i$ = 13.5 years [45] (Table 1), and (ii) the corrosion effects are considered at different times (construction time and after 13.5, 25, 50 and 75 years of bridge service life) to evaluate the variation of the seismic performance of the bridge over time. Moreover, (iii) the parameters shown in Table 2 are kept constant during the different corrosion scenarios.

Table 1. Initiation time $t_i$ as a function of *w/c* ratio.

| *w/c* | **Probability 99% [years]** | **Probability 50% [years]** |
|---|---|---|
| 0.4 | 61.7 | 60.4 |
| 0.5 | 26.3 | 26.0 |
| 0.6 | 13.7 | 13.5 |

Table 2. Constant parameters in the three different corrosion levels.

| Concrete compressive strength $f_{ck}$ | Initiation time $t_i$ | Penetration rate coefficient $k$ | Steel rebar ultimate deformation $\varepsilon_{u,0}$ |
|---|---|---|---|
| [MPa] | [year] | [-] | [%] |
| 28 | 13.5 | 0.0116 | 9 |

In the considered approach, the influence of corrosion on the mechanical properties of both steel and concrete is disregarded [48], limiting its effect on the reduction of steel rebars area.
To evaluate the seismic performance of the bridges, the modal pushover approach was chosen. The Capacity Spectrum Method (CSM) was adopted to determine the performance point of the structure [49,50,51,52]. In this approach, several capacity curves are obtained and for each of them, corresponding to a vibration mode shape with a participating mass greater than 1% and a modal loading profile, the performance point is calculated considering the relevant seismic demand spectrum. Consequently, for each considered vibration mode, it is possible to evaluate the internal actions for each monitored structural element in correspondence to the determined performance point. These actions are finally combined considering the complete quadratic combination (CQC) rule, for safety verification purposes.



## 3. Bridge case studies

The approach described in Section 2 was used to analyse the evolution over time of the collapse mechanisms of five existing RC motorway bridges subjected to seismic actions. These bridges were built around the 1960's and they are located in moderate to high seismicity regions of Northern Italy. The main seismic parameters that characterize the different sites are listed in Table 3.

Table 3. Main seismic parameters of the sites.

| | Soil type | PGA |
|---|---|---|
| | [-] | [g] |
| Bridge 1 | C | 0.166 |
| Bridge 2 | C | 0.156 |
| Bridge 3 | C | 0.152 |
| Bridge 4 | C | 0.158 |
| Bridge 5 | C | 0.079 |

The first three bridges are characterized by hollow section RC hammered piers while the last two are supported by framed RC piers, with rectangular pillars. The description of the pier cross sections (including geometry, materials, and reinforcement) can be found in Tables 4 and 5. All the bridges are characterized by simply supported spans on elastomeric bearings. Particularly interesting is Bridge 4 which includes a roofing slab running over the deck, to protect the carriageway from intense snowing storms (it is located in a mountain region). The number of spans ranges from 4 (Bridge 2) to 15 (Bridge 3) and all the decks are composed of precast prestressed RC longitudinal beams with transverse beams and a RC slab. The length of the spans is about 40-41 m for the first two Bridges,

while between 30 and 35 m for Bridges 3 and 5. Given the particularity of the geometry, Bridge 4 is characterized by significantly lower spans (around 19 m). The width of the deck is related to the number of traffic lanes hosted by the bridge, commonly two plus an additional one reserved for emergency. Thus, the widths are around 10 m for the first three Bridges and around 11 m for the last two Bridges.
All the bridges are characterized by a limited longitudinal slope of the decks. The planar configuration is almost straight, except for Bridges 4 and 5 which are characterized by the beginning of a turn at one end (Fig. 6).
The fundamental structural properties of the bridges are summarized in Table 4 and the characteristics of the piers are reported in Table 5. It is important to notice that all the five case studies present poor construction details that are typical of RC bridges built in Italy in those years.

Table 4. Structural characteristics of the analysed bridges.

| | Type [-] | Spans [n°] | Bridge length [m] | Bearings for pier [n°] | Bearings type [-] | Piers [n°] | Piers shape [-] | Piers Thickness [m] | Concrete Strength $f_{ck}$ [MPa] | Steel Strength $f_{yk}$ [MPa] |
|---|---|---|---|---|---|---|---|---|---|---|
| Bridge 1 | Multi-span | 9 | 367 | 6 | Elastomeric | 8 | Rectangular hollow | 0.30 | 28 | 440 |
| Bridge 2 | Multi-span | 4 | 200 | 6 | Elastomeric | 3 | Hexagonal hollow | 0.35 | 28 | 440 |
| Bridge 3 | Multi-span | 15 | 515 | 6 | Elastomeric | 14 | Rectangular hollow | 0.35 | 28 | 440 |
| Bridge 4 | Multi-span | 8 | 152 | 12 | Elastomeric | 7 | Rectangular | - | 28 | 440 |
| Bridge 5 | Multi-span | 8 | 282 | 6 | Elastomeric | 7 | Rectangular | - | 28 | 440 |



Table 5. Characteristics of the piers.

| Bridge 1 | | | | | Bridge 2 | | | | |
|---|---|---|---|---|---|---|---|---|---|
| | Dimensions [m] | Height [m] | Longitudinal rebars [-] | Stirrups [-] | | Dimensions [m] | Height [m] | Longitudinal rebars [-] | Stirrups [-] |
| Pier 1 | 7.0 × 4.5 | 20.63 | 328Ø16 | Ø8/30 | Pier 1 | 4.0 × 2.5 | 5.06 | 148Ø14 | Ø10/20 |
| Pier 2 | 7.0 × 4.5 | 39.33 | 328Ø16 | Ø8/30 | Pier 2 | 4.0 × 2.5 | 10.84 | 148Ø14 | Ø10/20 |
| Pier 3 | 7.0 × 4.5 | 53.02 | 328Ø16 | Ø8/30 | Pier 3 | 4.0 × 2.5 | 15.51 | 148Ø14 | Ø10/20 |
| Pier 4 | 7.0 × 4.5 | 49.82 | 328Ø16 | Ø8/30 | Bridge 4 | | | | |
| Pier 5 | 7.0 × 4.5 | 46.02 | 328Ø16 | Ø8/30 | Pier 1 | 1.30 × 0.50 | 6.60 | 20Ø16 | Ø8/30 |
| Pier 6 | 7.0 × 4.5 | 51.13 | 328Ø16 | Ø8/30 | Pier 2 | 1.30 × 0.50 | 9.50 | 20Ø16 | Ø8/30 |
| Pier 7 | 7.0 × 4.5 | 34.40 | 328Ø16 | Ø8/30 | Pier 3 | 1.90 × 0.35 | 14.56 | 24Ø16 | Ø8/30 |
| Pier 8 | 7.0 × 4.5 | 14.26 | 328Ø16 | Ø8/30 | Pier 4 | 1.90 × 0.50 | 25.06 | 24Ø16 | Ø8/30 |
| Bridge 3 | | | | | Pier 5 | 1.90 × 0.50 | 34.90 | 24Ø16 | Ø8/30 |
| Pier 1 | 8.0 × 3.3 | 14.50 | 164Ø14 | Ø10/20 | Pier 6 | 1.90 × 0.50 | 34.90 | 24Ø16 | Ø8/30 |
| Pier 2 | 8.0 × 3.3 | 18.50 | 164Ø14 | Ø10/20 | Pier 7 | 1.90 × 0.35 | 15.90 | 24Ø16 | Ø8/30 |
| Pier 3 | 8.0 × 3.3 | 28.53 | 164Ø14 | Ø10/20 | Bridge 5 | | | | |
| Pier 4 | 8.0 × 3.3 | 37.00 | 164Ø14 | Ø10/20 | Pier 1 | 2.30 × 0.90 | 2.73 | 8Ø16 | Ø8/20 |
| Pier 5 | 8.0 × 3.3 | 43.00 | 164Ø14 | Ø10/20 | Pier 2 | 1.02 × 0.72 | 10.47 | 12Ø18 | Ø12/40 |
| Pier 6 | 8.0 × 3.3 | 48.00 | 164Ø14 | Ø10/20 | Pier 3 | 0.92 × 0.72 | 15.95 | 12Ø16 | Ø12/40 |
| Pier 7 | 8.0 × 3.3 | 53.00 | 164Ø14 | Ø10/20 | Pier 4 | 0.80 × 0.60 | 21.70 | 6Ø18 | Ø12/40 |
| Pier 8 | 8.0 × 3.3 | 51.97 | 164Ø14 | Ø10/20 | Pier 5 | 0.92 × 0.72 | 27.30 | 12Ø18 | Ø12/40 |
| Pier 9 | 8.0 × 3.3 | 34,76 | 164Ø14 | Ø10/20 | Pier 6 | 0.92 × 0.72 | 14.21 | 12Ø16 | Ø12/40 |
| Pier 10 | 8.0 × 3.3 | 18.46 | 164Ø14 | Ø10/20 | Pier 7 | 0.80 × 0.60 | 9.40 | 12Ø18 | Ø12/40 |
| Pier 11 | 8.0 × 3.3 | 16.31 | 164Ø14 | Ø10/20 | | | | | |
| Pier 12 | 8.0 × 3.3 | 15.98 | 164Ø14 | Ø10/20 | | | | | |
| Pier 13 | 8.0 × 3.3 | 12.75 | 164Ø14 | Ø10/20 | | | | | |
| Pier 14 | 8.0 × 3.3 | 10.46 | 164Ø14 | Ø10/20 | | | | | |

Fig. 6 shows the finite element models of the considered case studies. The FEMs of the five bridges involve 285, 50, 160, 713, and 541 respectively. Particularly, the number of finite elements used for the modelling of the tallest pier of each bridge is 13, 7, 7, 48, and 118 respectively. The first three fundamental periods characterizing the dynamic behaviour of the five bridges are reported in Table 6.

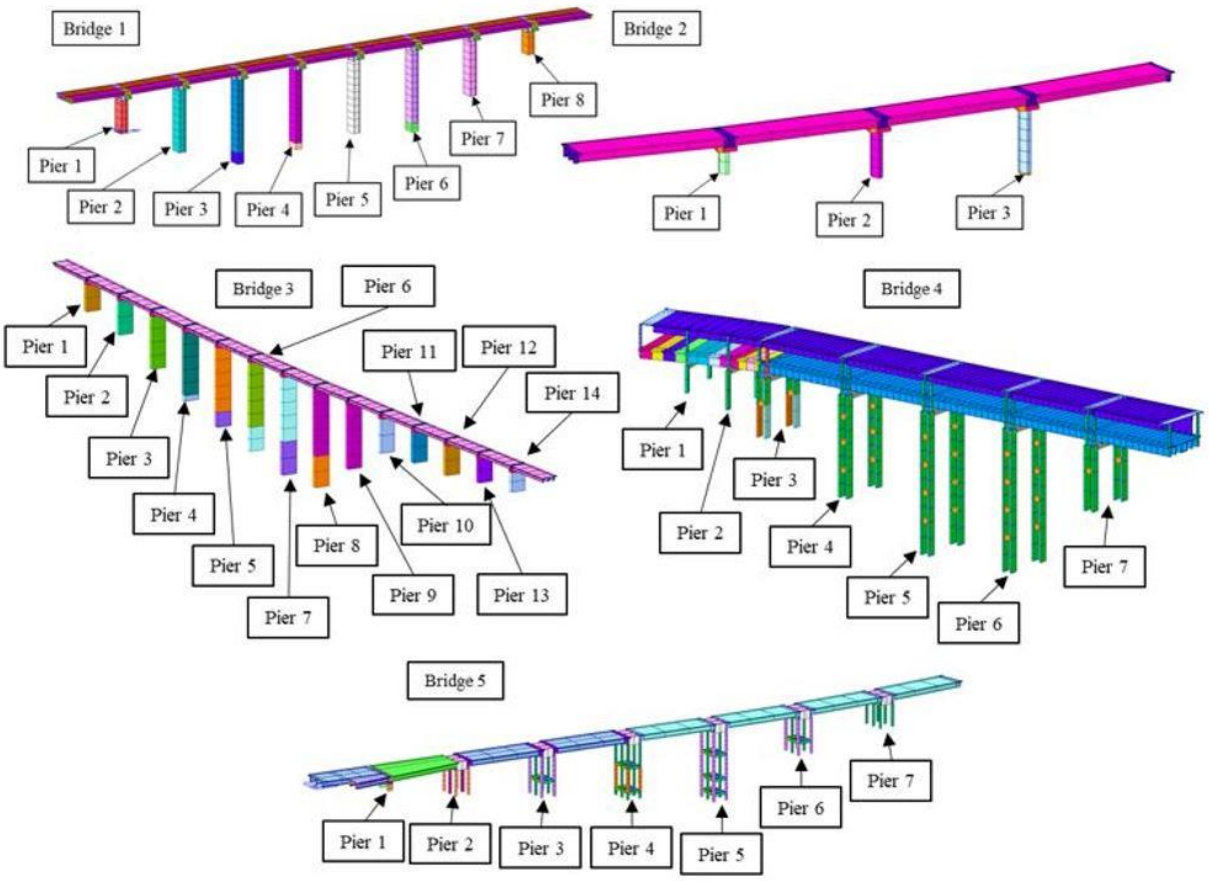


Figure 6. FEMs of the bridges.

Table 6. First three fundamental periods of the bridges under study.

| | $T_1$ | $T_2$ | $T_3$ |
|---|---|---|---|
| | [s] | [s] | [s] |
| Bridge 1 | 2.73 | 2.56 | 2.41 |
| Bridge 2 | 1.23 | 1.16 | 0.94 |
| Bridge 3 | 2.69 | 1.91 | 1.79 |
| Bridge 4 | 2.47 | 1.37 | 1.15 |
| Bridge 5 | 4.39 | 3.16 | 3.09 |

Table 7 presents the corrosion effects on steel reinforcements in terms of progressive diameter and area reductions as a function of the age of the bridge, for both longitudinal and transverse steel reinforcements, and different corrosion levels (estimated on the basis of Eqs. (4)-(5)).

Table 7. Corrosion effects on steel reinforcement.

| $t$ | Slight Corrosion | | | | Moderate Corrosion | | | | High Corrosion | | | |
|---|---|---|---|---|---|---|---|---|---|---|---|---|
| | $i_{corr}$ = 0.1 [μA/cm$^2$] | | | | $i_{corr}$ = 1 [μA/cm$^2$] | | | | $i_{corr}$ = 5 [μA/cm$^2$] | | | |
| | $d_0$ | $d$ | $\Delta A_s$ | $\varepsilon_u$ | $d_0$ | $d$ | $\Delta A_s$ | $\varepsilon_u$ | $d_0$ | $d$ | $\Delta A_s$ | $\varepsilon_u$ |
| [year] | [mm] | [mm] | [%] | [%] | [mm] | [mm] | [%] | [%] | [mm] | [mm] | [%] | [%] |
| 0-13.5 | 8.00 | 8.00 | 0.00 | 9.00 | 8.00 | 8.00 | 0.00 | 9.00 | 8.00 | 8.00 | 0.00 | 9.00 |
| | 10.00 | 10.00 | 0.00 | 9.00 | 10.00 | 10.00 | 0.00 | 9.00 | 10.00 | 10.00 | 0.00 | 9.00 |
| | 12.00 | 12.00 | 0.00 | 9.00 | 12.00 | 12.00 | 0.00 | 9.00 | 8.00 | 8.00 | 0.00 | 9.00 |
| | 14.00 | 14.00 | 0.00 | 9.00 | 14.00 | 14.00 | 0.00 | 9.00 | 14.00 | 14.00 | 0.00 | 9.00 |
| | 16.00 | 16.00 | 0.00 | 9.00 | 16.00 | 16.00 | 0.00 | 9.00 | 16.00 | 16.00 | 0.00 | 9.00 |
| | 18.00 | 18.00 | 0.00 | 9.00 | 18.00 | 18.00 | 0.00 | 9.00 | 18.00 | 18.00 | 0.00 | 9.00 |
| 25 | 8.00 | 7.97 | 0.33 | 8.94 | 8.00 | 7.73 | 3.34 | 8.42 | 8.00 | 6.67 | 16.68 | 6.07 |
| | 10.00 | 9.97 | 0.27 | 8.95 | 10.00 | 9.73 | 2.67 | 8.53 | 10.00 | 8.67 | 13.34 | 6.66 |
| | 12.00 | 11.97 | 0.22 | 8.95 | 12.00 | 11.73 | 2.22 | 8.52 | 12.00 | 10.67 | 11.12 | 6.72 |
| | 14.00 | 13.97 | 0.19 | 8.97 | 14.00 | 13.73 | 1.91 | 8.67 | 14.00 | 12.67 | 9.53 | 7.33 |
| | 16.00 | 15.97 | 0.17 | 8.97 | 16.00 | 15.73 | 1.67 | 8.71 | 16.00 | 14.67 | 8.34 | 7.54 |
| | 18.00 | 17.97 | 0.15 | 8.98 | 18.00 | 17.73 | 1.48 | 8.81 | 18.00 | 16.67 | 7.41 | 7.62 |
| 50 | 8.00 | 7.93 | 0.91 | 8.87 | 8.00 | 7.27 | 9.14 | 7.71 | 8.00 | 4.35 | 45.68 | 0.98 |
| | 10.00 | 9.93 | 0.73 | 8.90 | 10.00 | 9.27 | 7.31 | 7.97 | 10.00 | 6.35 | 36.54 | 2.59 |
| | 12.00 | 11.92 | 0.71 | 8.91 | 12.00 | 11.15 | 7.06 | 8.39 | 12.00 | 7.77 | 35.28 | 2.83 |
| | 14.00 | 13.93 | 0.52 | 8.93 | 14.00 | 13.27 | 5.22 | 8.26 | 14.00 | 10.35 | 26.10 | 4.42 |
| | 16.00 | 15.93 | 0.46 | 8.94 | 16.00 | 15.27 | 4.57 | 8.36 | 16.00 | 12.35 | 22.84 | 4.99 |
| | 18.00 | 17.93 | 0.46 | 8.95 | 18.00 | 17.27 | 4.05 | 8.46 | 18.00 | 14.35 | 20.27 | 5.33 |
| 75 | 8.00 | 7.86 | 1.78 | 8.69 | 8.00 | 6.57 | 17.84 | 5.87 | 8.00 | 0.87 | 89.18 | 0.37 |
| | 10.00 | 9.86 | 1.43 | 8.75 | 10.00 | 8.57 | 14.27 | 6.50 | 10.00 | 2.87 | 71.34 | 0.53 |
| | 12.00 | 11.86 | 1.19 | 8.78 | 12.00 | 10.57 | 11.89 | 6.45 | 12.00 | 4.87 | 59.45 | 0.67 |
| | 14.00 | 13.86 | 1.02 | 8.82 | 14.00 | 12.57 | 10.19 | 7.21 | 14.00 | 6.87 | 50.96 | 0.72 |
| | 16.00 | 15.86 | 0.89 | 8.84 | 16.00 | 14.57 | 8.92 | 7.44 | 16.00 | 8.87 | 44.59 | 1.18 |
| | 18.00 | 17.86 | 0.79 | 8.91 | 18.00 | 16.57 | 7.93 | 8.05 | 18.00 | 10.87 | 39.63 | 2.50 |



As mentioned in Section 2, the corrosion effects start after 13.5 years since the construction of the structure and consequently, before that time, the effects in terms of area reduction of the steel reinforcements are not present. Considering 25 years after the construction of the bridges, the steel reinforcements area reduction is significant only in the case of high corrosion scenario ($i_{corr}$ = 5 μA/cm$^2$) where it also reaches values higher than 10% for 8 mm, 10 mm, and 12 mm rebar diameters, whereas for 14 mm, 16 mm, and 18 mm rebar diameters the obtained area reduction is 9.53%, 8.34%, and 7.41%, respectively.

In the case of 50 years after the construction of the structures, the area reduction becomes significant also for the moderate corrosion scenario, characterized by a corrosion current density equal to 1 μA/cm$^2$. In fact, the results show values of steel reinforcements area reduction between 4% and 10%. The high corrosion scenario, instead, is characterized by reductions greater than 20% for all the rebar diameters.

After 75 years from the construction of the bridges, the corrosion effects significantly increase showing steel reinforcements area reduction values greater than 40% considering the high corrosion scenario. Particular attention must be paid to the stirrups, generally characterized by low steel rebar diameter (8 mm and 10 mm in this work), where the carbonation phenomenon leads to area reduction greater than 70%. For the moderate corrosion scenario, the steel reinforcements area reduction is equal to 11.89%, 10.19%, 8.92%, and 7.93% for rebar diameters equal to 12 mm, 14 mm, 16 mm, and 18 mm, respectively. For the steel stirrups, having diameter of 8 mm or 10 mm, the area reduction is 17.84% and 14.27%, respectively.

Furthermore, the slight corrosion scenario ($i_{corr}$ = 0.1 μA/cm$^2$) leads to very low values of steel rebars area reduction which does not exceed 2% also after 75 years after the construction of the structure.

Figs. 7, 8, 9, 10, and 11 show the trend of the moment-curvature diagram of the base cross-section of Pier 1 of Bridges 1, 2, 3, 4 and of Pier 4 of Bridge 5 for all the corrosion scenarios analysed in this work. According to the above considerations, the maximum moment of the cross-section significantly decreases as a function of both the age of the structure and the corrosion level. This is more evident in the case of high corrosion scenario, whereas for the slight corrosion level the variation of the maximum moment is very low. It is possible to notice that after 25 years from the construction of the bridges, the moment-curvature diagrams evaluated in slight and moderate corrosion levels are practically coincident, given the low difference in terms of steel reinforcements area reduction. The moment-curvature diagrams evaluated at 0 and 13.5 years are not represented in Figs. 7, 8, 9, 10, and 11 because they are practically coincident with the corresponding ones related to the slight corrosion level.

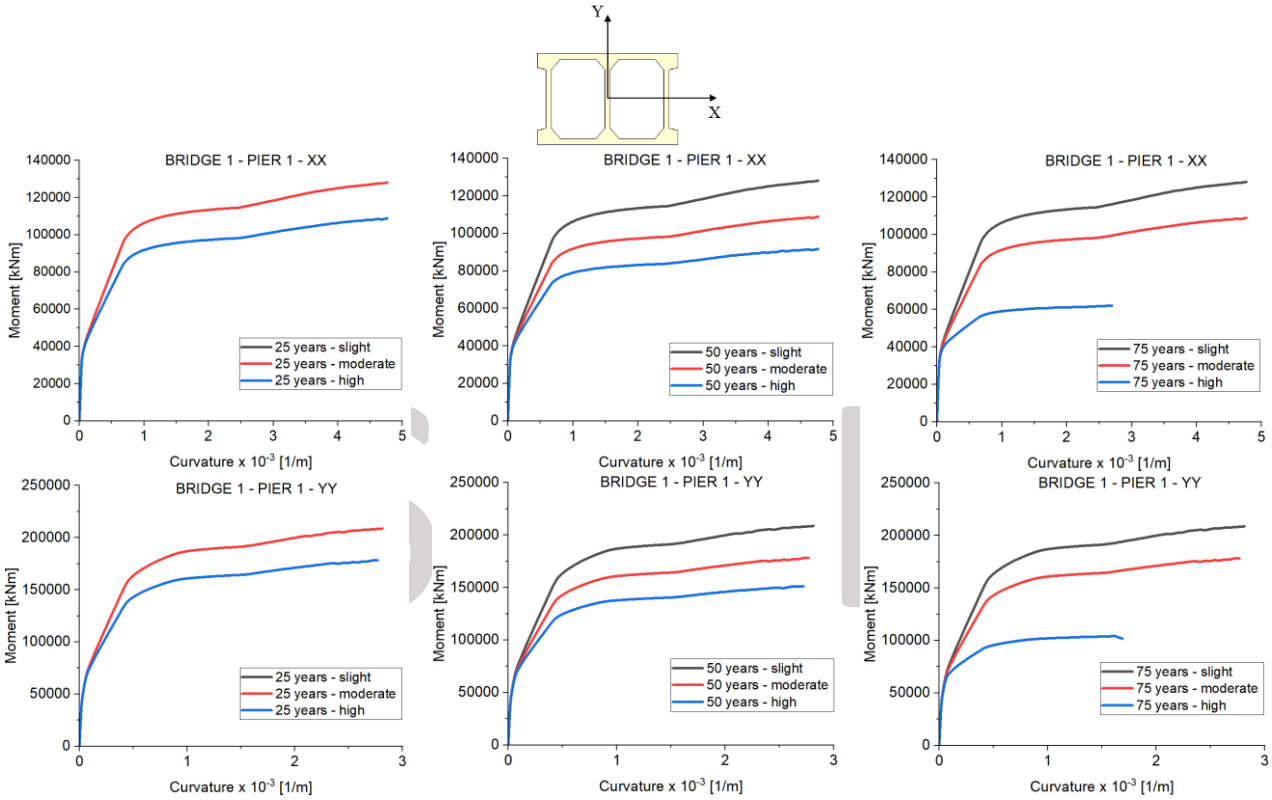


Figure 7. Moment-curvature diagram for Pier 1 of Bridge 1 for all the corrosion scenarios.

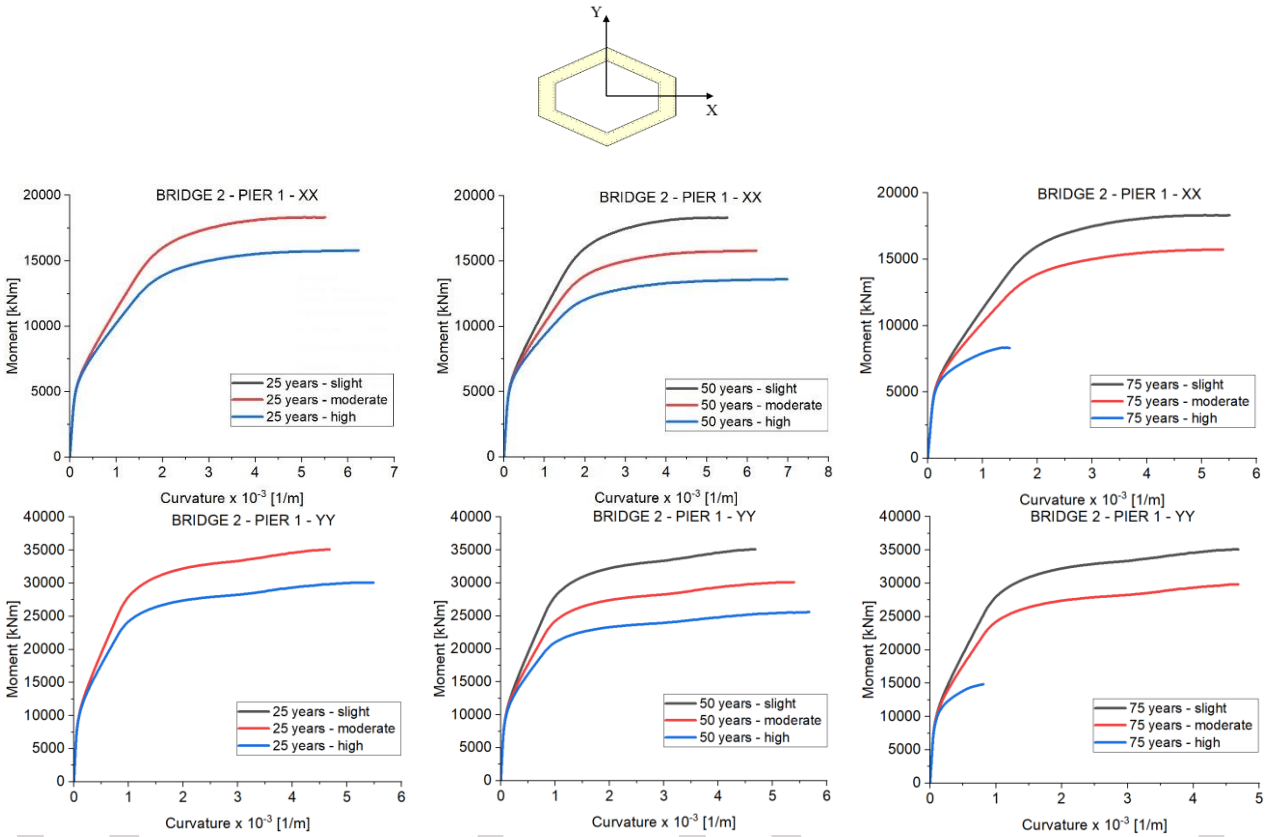


Figure 8. Moment-curvature diagram for Pier 1 of Bridge 2 for all the corrosion scenarios.



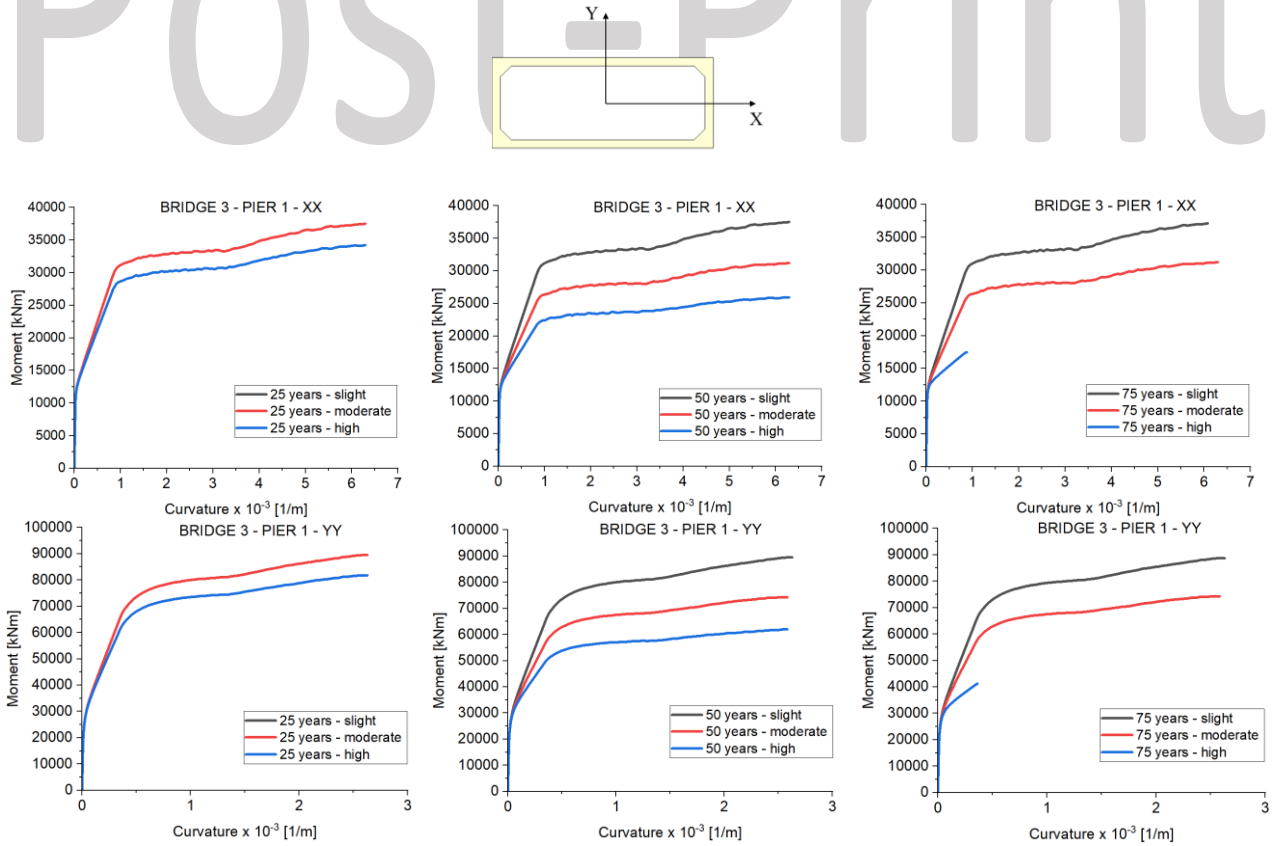


Figure 9. Moment-curvature diagram for Pier 1 of Bridge 3 for all the corrosion scenarios.

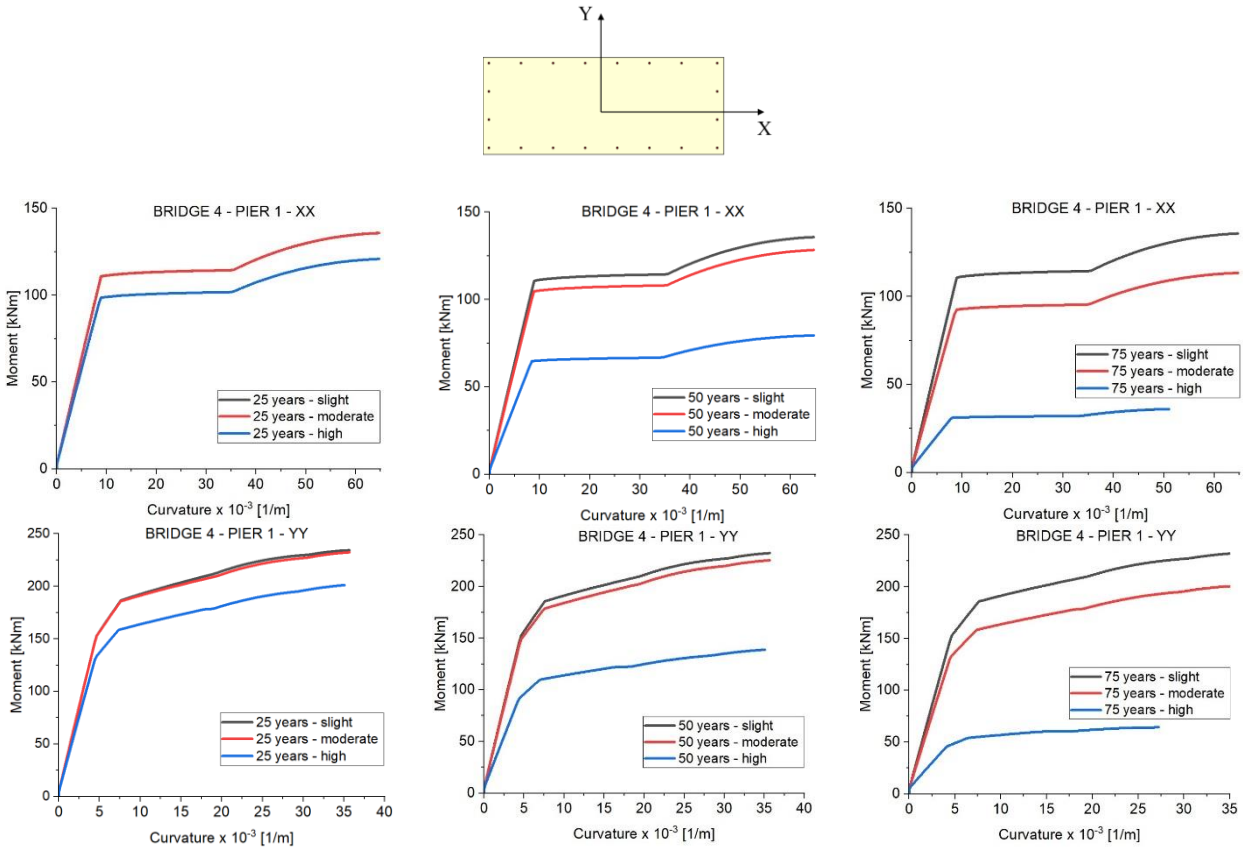


Figure 10. Moment-curvature diagram for Pier 1 of Bridge 4 for all the corrosion scenarios.



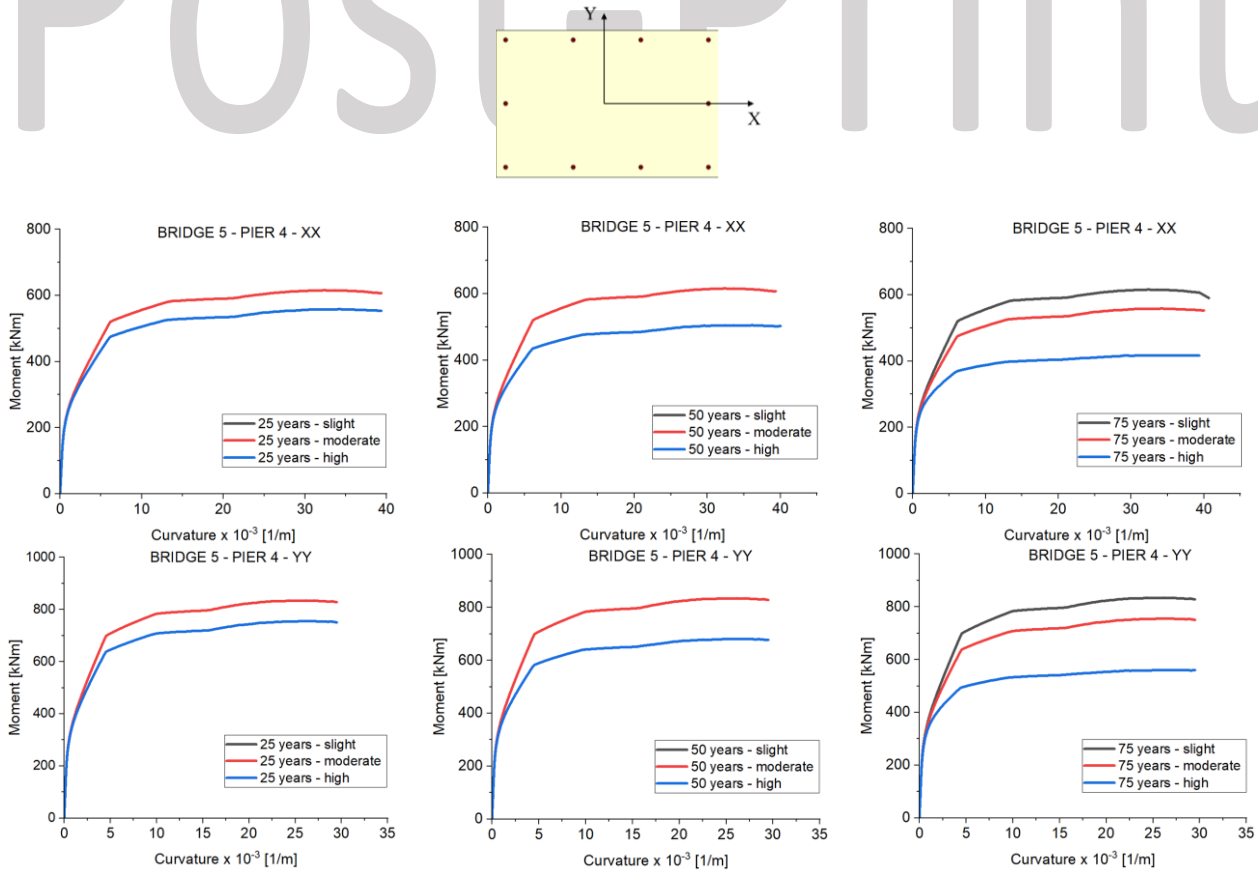


Figure 11. Moment-curvature diagram for Pier 4 of Bridge 5 for all the corrosion scenarios.

Figs. 7, 8, 9, 10 and 11 clearly show the influence of corrosion effects on the bearing capacity and ductility of piers cross-section as a function of the bridges age. The correlation between the bridges age and the corrosion amount can be found in Table 7.
As a result of the corrosion process, the stiffness of the piers progressively decreases. Consequently, a slight increase of the natural periods of the structure is obtained, especially referred to the first vibration modes. As an example, Fig. 12 summarizes the trend of the main vibration modes for Bridge 1.

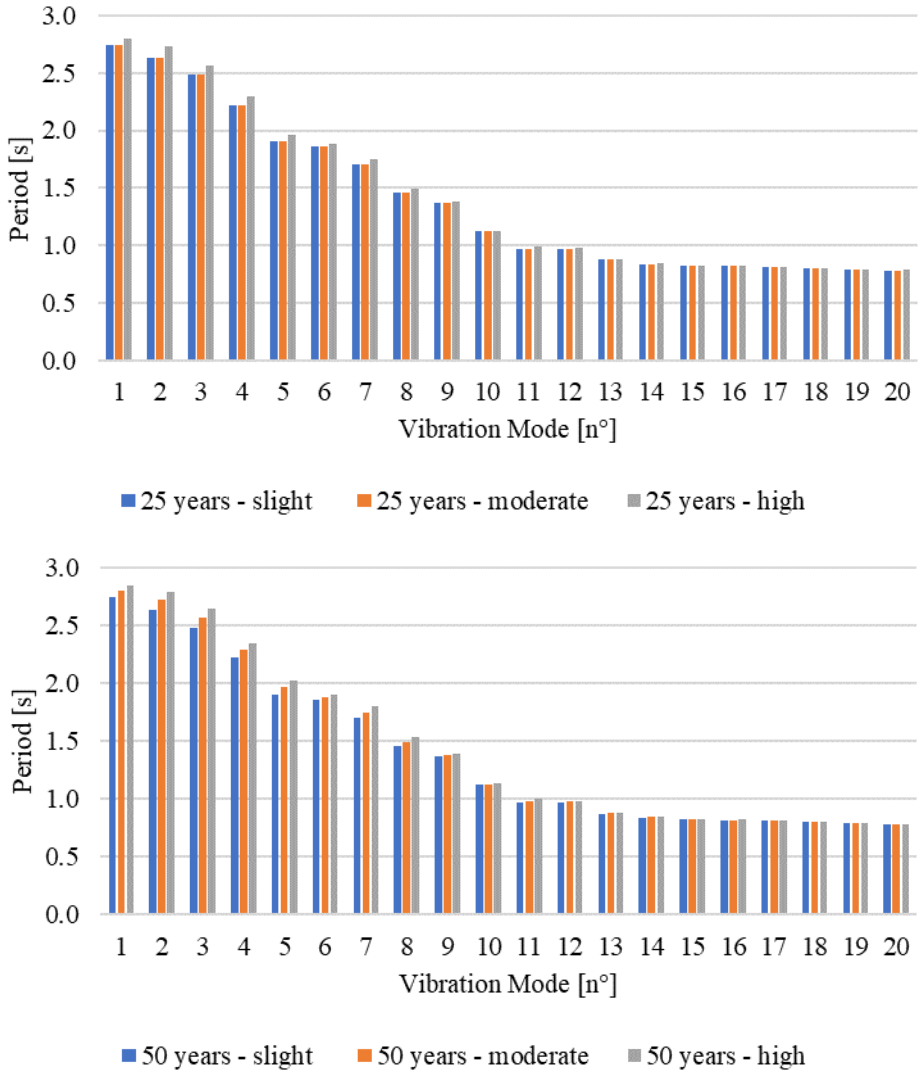

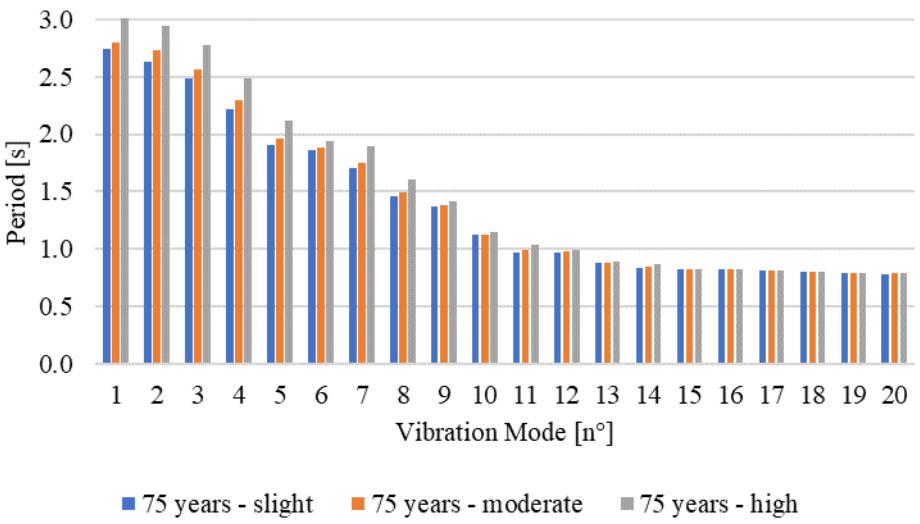


Figure 12. Variation of the first twenty natural periods of Bridge 1.

Furthermore, in addition to a slight increase of the first periods, it is worth noticing some slight differences in terms of deformed shapes, especially for vibration modes characterized by low periods. Finally, the capacity curves for each significant vibration mode are calculated according to the method presented in Section 2. Figs. 13-22 show the capacity curves for the first vibration mode shape of all the bridges, evaluated for all the corrosion scenarios, and for both the considered failure mechanisms (ductile and brittle).



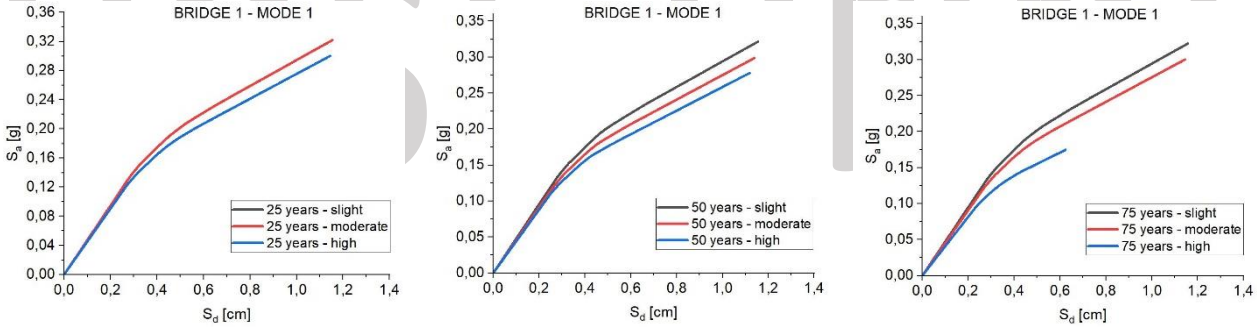


Figure 13. Capacity curves: ductile collapse mechanism, Bridge 1, mode 1.

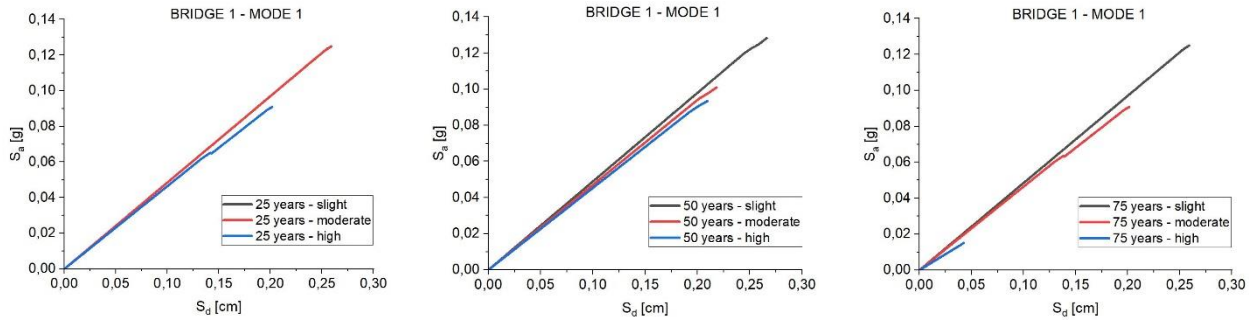


Figure 14. Capacity curves: brittle collapse mechanism, Bridge 1, mode 1.

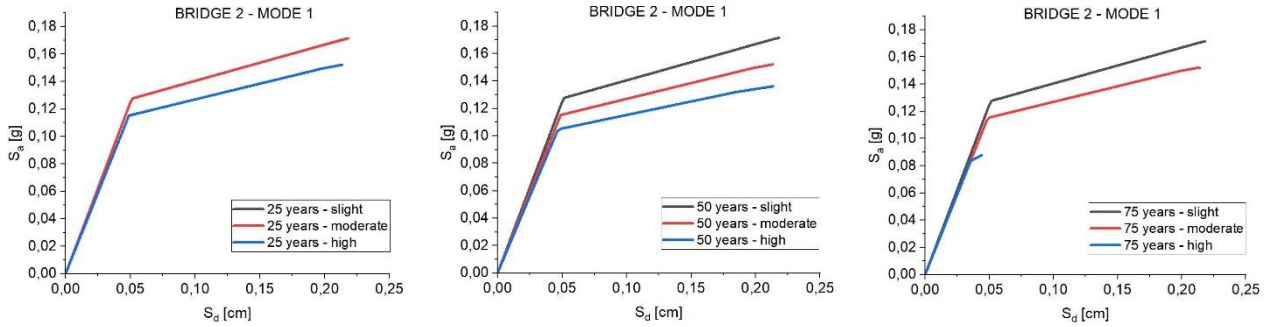


Figure 15. Capacity curves: ductile collapse mechanism, Bridge 2, mode 1.

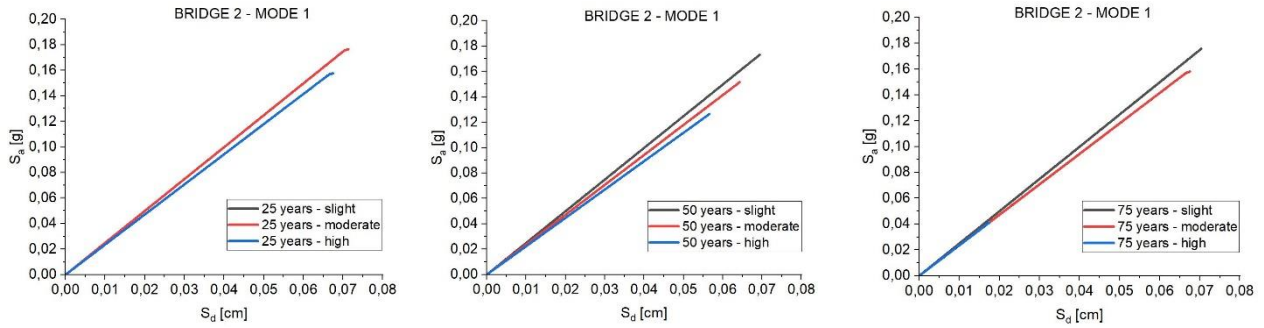


Figure 16. Capacity curves: brittle collapse mechanism, Bridge 2, mode 1.

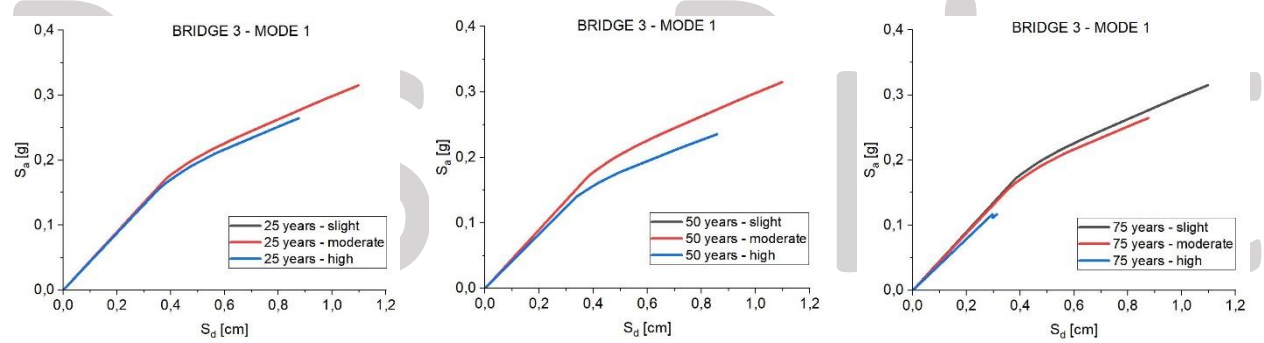


Figure 17. Capacity curves: ductile collapse mechanism, Bridge 3, mode 1.

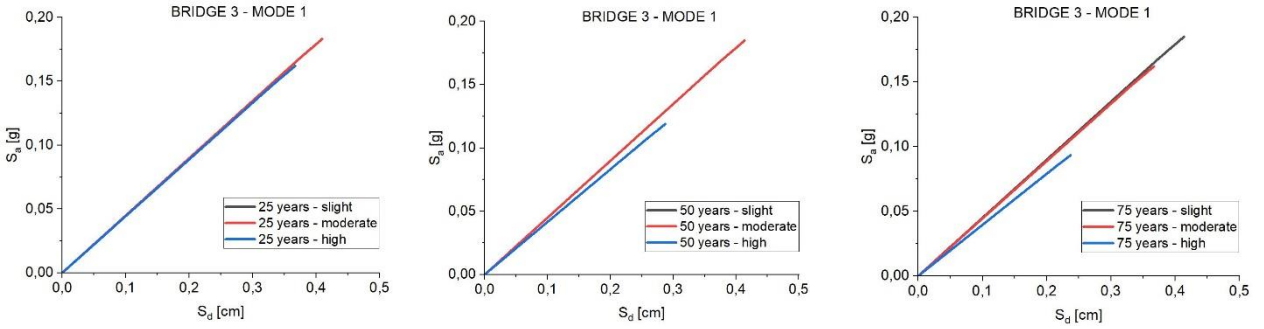


Figure 18. Capacity curves: brittle collapse mechanism, Bridge 3, mode 1.

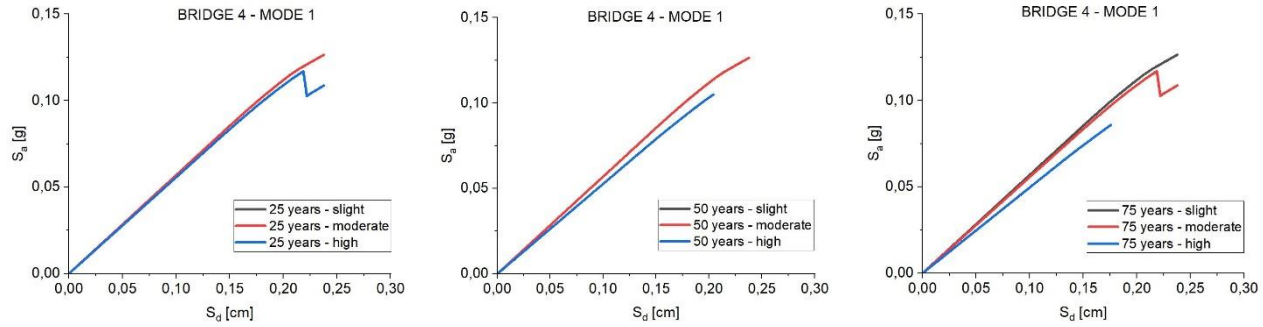


Figure 19. Capacity curves: ductile collapse mechanism, Bridge 4, mode 1.

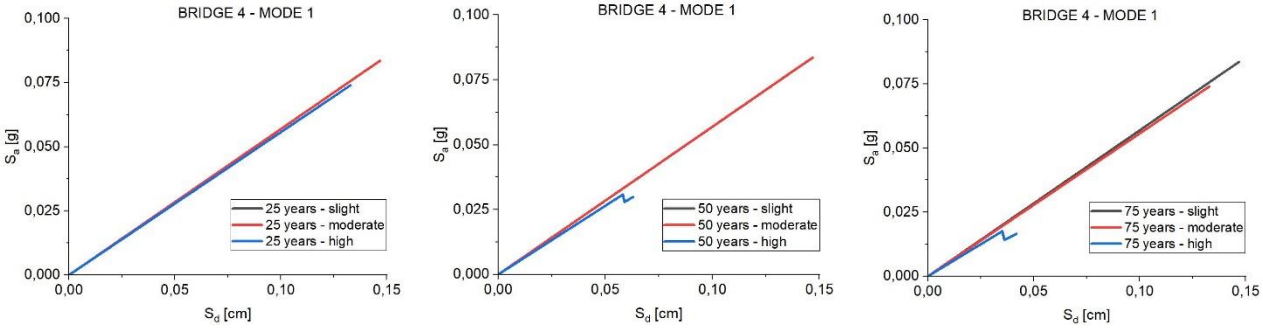


Figure 20. Capacity curves: brittle collapse mechanism, Bridge 4, mode 1.

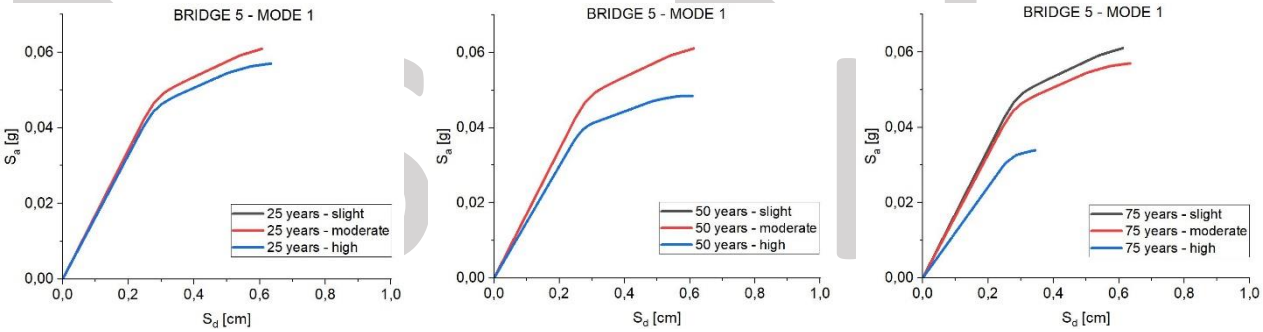


Figure 21. Capacity curves: ductile collapse mechanism, Bridge 5, mode 1.

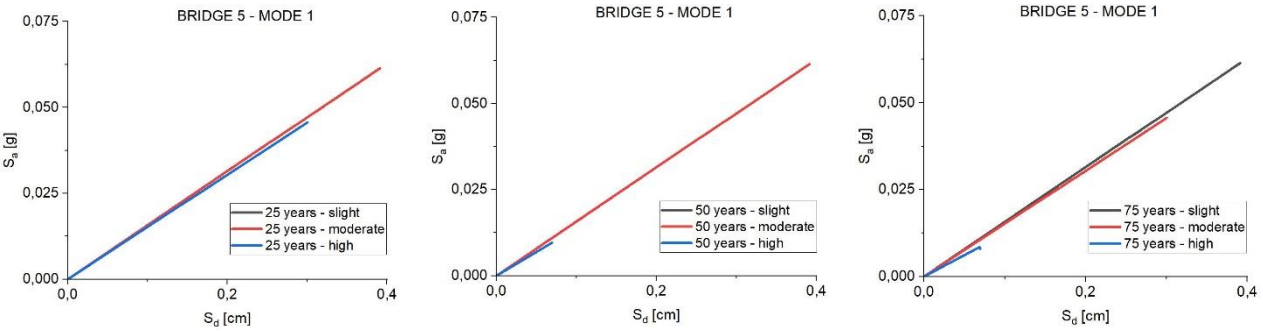


Figure 22. Capacity curves: brittle collapse mechanism, Bridge 5, mode 1.

It is possible to notice that, after 25 years from the construction, the capacity curves obtained for the slight and moderate corrosion scenarios are practically coincident because, according to the above-mentioned considerations, the moment-curvature diagrams of base cross-sections of the piers, and consequently the properties of the plastic hinges, do not change. Also in these diagrams, the corrosion scenarios concerning the initial construction time and after 13.5 years have not been plotted because their capacity curves overlap the ones obtained for the slight corrosion level.

Moreover, as regards the cases of 25-year-old and 50-year-old bridges, some curves appear overlapped in presence of slight and moderate corrosion levels. This result could be explained

considering that, as it is possible to notice in Table 7, the reduction of the steel reinforcement diameter does not differ significantly considering the two scenarios. This is more evident in presence of larger steel rebar diameters, where the steel reinforcement diameter reduction due to corrosion effects is less important. Furthermore, the capacity curves combine the behaviour of different piers (with different moment-curvature diagrams) under the same loading profile.

To complete the seismic performance evaluation of the considered bridges, modal pushover analyses have been performed following an iterative process through the increase of the demand spectrum up to the achievement of the required limit state.

After the determination of both the peak ground acceleration that leads to the collapse of the first structural element ($PGA_C$) and the related return period ($T_{R,C}$), it is possible to evaluate the risk indices with the following equations:

$$RI_{PGA} = \frac{PGA_C}{PGA_D} \tag{6}$$

$$RI_{TR} = \left(\frac{T_{R,C}}{T_{R,D}}\right)^{0.41} \tag{7}$$

where $PGA_D$ is the design peak ground acceleration, reported in Table 3, and $T_{R,D}$ is the corresponding return period, for the considered limit state [38].

The risk indices close or greater than one concern cases of safe bridges, whereas values smaller than one indicate structures with a high risk of seismic failure [53-55].

Tables 8, 9, 10, 11 and 12 summarize the obtained results in terms of risk indices considering the different corrosion scenarios and the two different collapse mechanisms. The results obtained considering 0 and 13.5 years are not reported in Tables 8, 9, 10, 11, and 12 because they are practically coincident with the corresponding ones calculated for the slight corrosion level.



Table 8. Risk indices values obtained for Bridge 1.

| Bridge 1 | Corrosion Scenario | Ductile Mechanism | | | | | |
|---|---|---|---|---|---|---|---|
| | | 25 years | | 50 years | | 75 years | |
| | | X | Y | X | Y | X | Y |
| $RI_{PGA}$ | **Slight** | **5.342** | **3.936** | **5.342** | **3.936** | **5.342** | **3.936** |
| | **Moderate** | **5.342 (0.00%)** | **3.936 (0.00%)** | **5.212 (-4.05%)** | **3.858 (-2.64%)** | **5.083 (-4.84%)** | **3.801 (-3.43%)** |
| | **High** | **5.083 (-4.84%)** | **3.801 (-3.43%)** | **4.968 (-7.00%)** | **3.782 (-4.56%)** | **3.194 (-40.21%)** | **2.348 (-40.35%)** |
| $RI_{TR}$ | **Slight** | **9.804** | **6.464** | **9.804** | **6.464** | **9.804** | **6.464** |
| | **Moderate** | **9.804 (0.00%)** | **6.464 (0.00%)** | **9.480 (-3.30%)** | **6.307 (-2.43%)** | **9.322 (-4.92%)** | **6.208 (-3.96%)** |
| | **High** | **9.322 (-4.92%)** | **6.208 (-3.96%)** | **8.879 (-9.34%)** | **6.122 (-5.29%)** | **4.862 (-50.41%)** | **3.198 (-50.53%)** |
| | | Brittle Mechanism | | | | | |
| $RI_{PGA}$ | **Slight** | **1.379** | **0.959** | **1.379** | **0.959** | **1.379** | **0.959** |
| | **Moderate** | **1.379 (0.00 %)** | **0.959 (0.00 %)** | **1.144 (-17.04%)** | **0.632 (-34.09%)** | **1.003 (-27.26%)** | **0.413 (-56.93%)** |
| | **High** | **1.003 (-27.26%)** | **0.413 (-56.93%)** | **0.937 (-32.05%)** | **0.299 (-68.82%)** | **0.442 (-67.95%)** | **0.241 (-74.87%)** |
| $RI_{TR}$ | **Slight** | **1.547** | **0.949** | **1.547** | **0.949** | **1.547** | **0.949** |
| | **Moderate** | **1.547 (0.00%)** | **0.949 (0.00%)** | **1.200 (-22.43%)** | **0.627 (-33.93%)** | **1.102 (-28.76%)** | **0.389 (-59.01)** |
| | **High** | **1.102 (-28.76%)** | **0.389 (-59.01%)** | **0.984 (-36.39%)** | **0.267 (-71.87%)** | **0.503 (-67.49%)** | **0.230 (-75.76%)** |

Table 9. Risk indices values obtained for Bridge 2.

| Bridge 2 | Corrosion Scenario | Ductile Mechanism | | | | | |
|---|---|---|---|---|---|---|---|
| | | 25 years | | 50 years | | 75 years | |
| | | X | Y | X | Y | X | Y |
| $RI_{PGA}$ | **Slight** | **2.091** | **2.169** | **2.091** | **2.169** | **2.091** | **2.169** |
| | **Moderate** | **2.091 (0.00%)** | **2.169 (0.00%)** | **2.001 (-4.30%)** | **1.975 (-8.94%)** | **2.001 (-4.30%)** | **1.975 (-8.94%)** |
| | **High** | **2.001 (-4.30%)** | **1.975 (-8.94%)** | **1.953 (-6.60%)** | **1.849 (-14.75%)** | **1.423 (-31.94%)** | **1.561 (-28.03%)** |
| $RI_{TR}$ | **Slight** | **2.645** | **2.776** | **2.645** | **2.776** | **2.645** | **2.776** |
| | **Moderate** | **2.645 (0.00%)** | **2.776 (0.00%)** | **2.515 (-5.03%)** | **2.453 (-11.64%)** | **2.515 (-5.03%)** | **2.453 (-11.64%)** |
| | **High** | **2.512 (-5.03%)** | **2.453 (-11.64%)** | **2.435 (-7.93%)** | **2.249 (-18.98%)** | **1.863 (-29.53%)** | **1.798 (-35.23%)** |
| | | Brittle Mechanism | | | | | |
| $RI_{PGA}$ | **Slight** | **1.048** | **0.874** | **1.048** | **0.874** | **1.048** | **0.874** |
| | **Moderate** | **1.048 (0.00%)** | **0.874 (0.00%)** | **0.827 (-21.09%)** | **0.794 (-9.15%)** | **0.807 (-22.99%)** | **0.735 (-15.90%)** |
| | **High** | **0.807 (-22.99%)** | **0.735 (-15.90%)** | **0.729 (-30.44%)** | **0.666 (-23.80%)** | **0.497 (-52.57%)** | **0.231 (-73.57%)** |
| $RI_{TR}$ | **Slight** | **1.063** | **0.854** | **1.063** | **0.854** | **1.063** | **0.854** |
| | **Moderate** | **1.063 (0.00%)** | **0.854 (0.00%)** | **0.800 (-24.74%)** | **0.742 (-13.11%)** | **0.797 (-25.02%)** | **0.682 (-20.14%)** |
| | **High** | **0.797 (-25.02%)** | **0.682 (-20.14%)** | **0.701 (-34.05%)** | **0.643 (-24.71%)** | **0.489 (-54.00%)** | **0.219 (-74.36%)** |

Table 10. Risk indices values obtained for Bridge 3.

| Bridge 3 | Corrosion Scenario | Ductile Mechanism | | | | | |
|---|---|---|---|---|---|---|---|
| | | 25 years | | 50 years | | 75 years | |
| | | X | Y | X | Y | X | Y |
| $RI_{PGA}$ | **Slight** | **4.873** | **5.531** | **4.873** | **5.531** | **4.873** | **5.531** |
| | **Moderate** | **4.873 (0.00%)** | **5.531 (0.00%)** | **4.873 (0.00%)** | **5.531 (0.00%)** | **4.813 (-1.20%)** | **4.683 (-15.30%)** |
| | **High** | **4.813 (-1.20%)** | **4.683 (-15.30%)** | **4.096 (-15.90%)** | **4.561 (-17.50)** | **3.273 (-32.80%)** | **3.797 (-31.40%)** |
| $RI_{TR}$ | **Slight** | **5.208** | **5.951** | **5.208** | **5.951** | **5.208** | **5.951** |
| | **Moderate** | **5.208 (0.00%)** | **5.951 (0.00%)** | **5.208 (0.00%)** | **5.951 (0.00%)** | **5.141 (-1.30%)** | **4.994 (-16.10%)** |
| | **High** | **5.141 (-1.30%)** | **4.994 (-16.10%)** | **4.338 (-16.70%)** | **4.858 (-18.40%)** | **3.479 (-33.20%)** | **4.167 (-30.00%)** |
| | | Brittle Mechanism | | | | | |
| $RI_{PGA}$ | **Slight** | **1.642** | **1.298** | **1.642** | **1.298** | **1.642** | **1.298** |
| | **Moderate** | **1.642 (0.00%)** | **1.298 (0.00%)** | **1.642 (0.00%)** | **1.298 (0.00%)** | **1.377 (-16.10%)** | **1.142 (-12.00%)** |
| | **High** | **1.377 (-16.10)** | **1.142 (-12.00%)** | **1.014 (-38.20%)** | **1.045 (-19.50%** | **0.532 (-67.60%)** | **0.882 (-32.00%)** |
| $RI_{TR}$ | **Slight** | **1.658** | **1.297** | **1.658** | **1.297** | **1.658** | **1.297** |
| | **Moderate** | **1.658 (0.00%)** | **1.297 (0.00%)** | **1.658 (0.00%)** | **1.297 (0.00%)** | **1.379 (-16.80%)** | **1.142 (-12.00%)** |
| | **High** | **1.379 (-16.80%)** | **1.142 (-12.00%)** | **1.014 (-38.80%)** | **1.044 (-19.50%)** | **0.602 (-63.70%)** | **0.896 (-30.90%)** |

Table 11. Risk indices values obtained for Bridge 4.

| Bridge 4 | Corrosion Scenario | Ductile Mechanism | | | | | |
|---|---|---|---|---|---|---|---|
| | | 25 years | | 50 years | | 75 years | |
| | | X | Y | X | Y | X | Y |
| $RI_{PGA}$ | **Slight** | **1.294** | **1.365** | **1.294** | **1.365** | **1.294** | **1.365** |
| | **Moderate** | **1.294 (0.00%)** | **1.365 (0.00%)** | **1.294 (0.00%)** | **1.365 (0.00%)** | **1.255 (-3.00%)** | **1.325 (-2.90%)** |
| | **High** | **1.255 (-3.00%)** | **1.325 (-2.90%)** | **1.174 (-9.30%)** | **1.313 (-3.80%)** | **1.067 (-17.50%)** | **1.100 (-19.40%)** |
| $RI_{TR}$ | **Slight** | **1.387** | **1.484** | **1.387** | **1.484** | **1.387** | **1.484** |
| | **Moderate** | **1.387 (0.00%)** | **1.484 (0.00%)** | **1.387 (0.00%)** | **1.484 (0.00%)** | **1.333 (-3.90%)** | **1.428 (-3.80%)** |
| | **High** | **1.333 (-3.90%)** | **1.428 (-3.80%)** | **1.225 (-11.70%)** | **1.412 (-4.90%)** | **1.085 (-21.80%)** | **1.127 (-24.10%)** |
| | | Brittle Mechanism | | | | | |
| $RI_{PGA}$ | **Slight** | **0.908** | **0.572** | **0.908** | **0.572** | **0.908** | **0.572** |
| | **Moderate** | **0.908 (0.00%)** | **0.572 (0.00%)** | **0.908 (0.00%)** | **0.572 (0.00%)** | **0.790 (-13.00%)** | **0.474 (-17.10%)** |
| | **High** | **0.790 (-13.00%)** | **0.474 (-17.10%)** | **0.266 (-70.70%)** | **0.414 (-27.60%)** | **0.229 (-74.80%)** | **0.214 (-62.60%)** |
| $RI_{TR}$ | **Slight** | **0.897** | **0.551** | **0.897** | **0.551** | **0.897** | **0.551** |
| | **Moderate** | **0.897 (0.00%)** | **0.551 (0.00%)** | **0.897 (0.00%)** | **0.551 (0.00%)** | **0.767 (-14.50%)** | **0.457 (-17.10%)** |
| | **High** | **0.767 (-14.50%)** | **0.457 (-17.10%)** | **0.278 (-69.00%)** | **0.408 (-26.00%)** | **0.244 (-72.80%)** | **0.231 (-58.10%)** |



Table 12. Risk indices values obtained for Bridge 5.

| Bridge 5 | Corrosion Scenario | Ductile Mechanism | | | | | |
|---|---|---|---|---|---|---|---|
| | | 25 years | | 50 years | | 75 years | |
| | | X | Y | X | Y | X | Y |
| $RI_{PGA}$ | **Slight** | **3.217** | **2.411** | **3.217** | **2.411** | **3.217** | **2.411** |
| | **Moderate** | **3.217 (0.00%)** | **2.411 (0.00%)** | **3.217 (0.00%)** | **2.411 (0.00%)** | **2.967 (-7.80%)** | **2.399 (-0.50%)** |
| | **High** | **2.967 (-7.80%)** | **2.399 (-0.50%)** | **2.899 (-9.90%)** | **2.322 (-2.70%)** | **2.701 (-16.00%)** | **2.116 (-12.20%)** |
| $RI_{TR}$ | **Slight** | **6.780** | **4.226** | **6.780** | **4.226** | **6.780** | **4.226** |
| | **Moderate** | **6.780 (0.00%)** | **4.226 (0.00%)** | **6.780 (0.00%)** | **4.226 (0.00%)** | **6.041 (-10.90%)** | **4.194 (-0.80%)** |
| | **High** | **6.041 (-10.90%)** | **4.194 (-0.80%)** | **5.764 (-15.00%)** | **3.973 (-6.00%)** | **5.091 (-24.90%)** | **3.412 (-19.30%)** |
| | | Brittle Mechanism | | | | | |
| $RI_{PGA}$ | **Slight** | **2.114** | **1.907** | **2.114** | **1.907** | **2.114** | **1.907** |
| | **Moderate** | **2.114 (0.00%)** | **1.907 (0.00%)** | **2.114 (0.00%)** | **1.907 (0.00%)** | **0.999 (-52.70%)** | **0.617 (-67.60%)** |
| | **High** | **0.999 (-52.70%)** | **0.617 (-67.60%)** | **0.673 (-68.20%)** | **0.399 (-79.10)** | **0.599 (-71.70%)** | **0.320 (-83.20%)** |
| $RI_{TR}$ | **Slight** | **3.407** | **2.877** | **3.407** | **2.877** | **3.407** | **2.877** |
| | **Moderate** | **3.407 (0.00%)** | **2.877 (0.00%)** | **3.407 (0.00%)** | **2.877 (0.00%)** | **1.001 (-70.60%)** | **0.515 (-82.10%)** |
| | **High** | **1.001 (-70.60%)** | **0.515 (-82.10%)** | **0.576 (-83.10%)** | **0.316 (-89.00%)** | **0.500 (-85.30%)** | **0.256 (-91.10%)** |

It is possible to underline that the reduction of the risk indices is more evident for the brittle collapse mechanism. In fact, considering the case of 75 years old bridges, the decrease of the risk index related to the brittle failure mechanism reaches values around 80%. This aspect is particularly relevant for the evaluation of the seismic vulnerability of existing RC bridges. In fact, the seismic vulnerability analysis results show risk indices values smaller than 1 at the initial construction time or considering slight corrosion scenario only for the brittle collapse mechanism. This is due to the poor construction details that characterize the transverse steel reinforcements of the existing RC bridges built in Italy around 1960's. On the contrary, the ductile collapse mechanism presents risk indices values greater than 1 for all the corrosion scenarios here analysed, even if showing reductions of the risk indices that reach 50% after 75 years from the construction time of the bridges, in the case of high corrosion level. The slight corrosion scenario does not influence the risk indices values evolution of both the collapse mechanisms over time due to the small reduction of the steel reinforcements area that characterizes this corrosion level.

After 25 years from the construction time of the bridges, the moderate corrosion scenario does not show a remarkable reduction of the risk indices values. In fact, the risk indices determined for both

the collapse mechanisms coincide with the ones obtained considering the slight corrosion level. On the contrary, the high corrosion level shows considerable reductions of the risk indices, especially considering the brittle collapse mechanism, which reaches reduction values even equal to 82% for the risk index of Bridge 5 evaluated in Y direction (transverse direction referred to the bridge axis).
After 50 years from the construction time of the bridges, even the moderate corrosion scenario leads to important reduction of the risk indices related to the brittle collapse mechanism, exceeding 79% in Y direction of Bridge 5. Moreover, the high corrosion scenario shows very important reduction values considering the brittle collapse mechanism.
After 75 years from the construction time of the bridges, both the moderate and high corrosion scenarios significantly affect the seismic vulnerability of the considered bridges. In fact, especially for the high corrosion level, the reduction of the risk indices appears considerable even for the ductile collapse mechanism, exceeding 30% for almost all cases.
Figs. 23, 24, 25, 26 and 27 summarize the evolution over time of the risk index expressed in terms of PGA and normalized with respect to the risk index initial value (obtained in the absence of corrosion). These results could be presented also in terms of risk index variation as a function of steel reinforcement area reduction. In the present work, the first way to plot the performance decrease was adopted because it is more suitable for managing and planning interventions by the owner of the infrastructure and stakeholders.

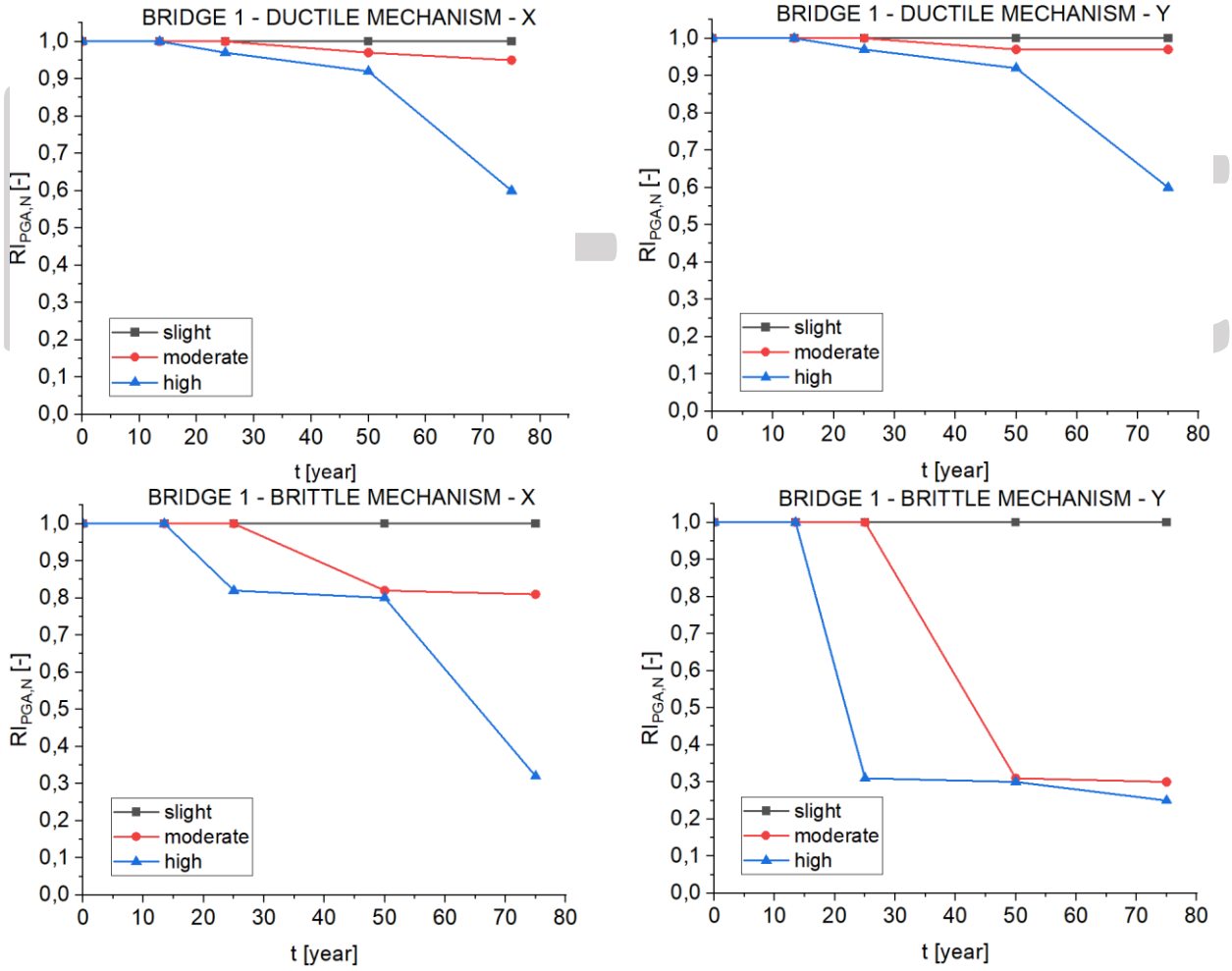


Figure 23. Evolution of the normalized PGA risk index, Bridge 1.

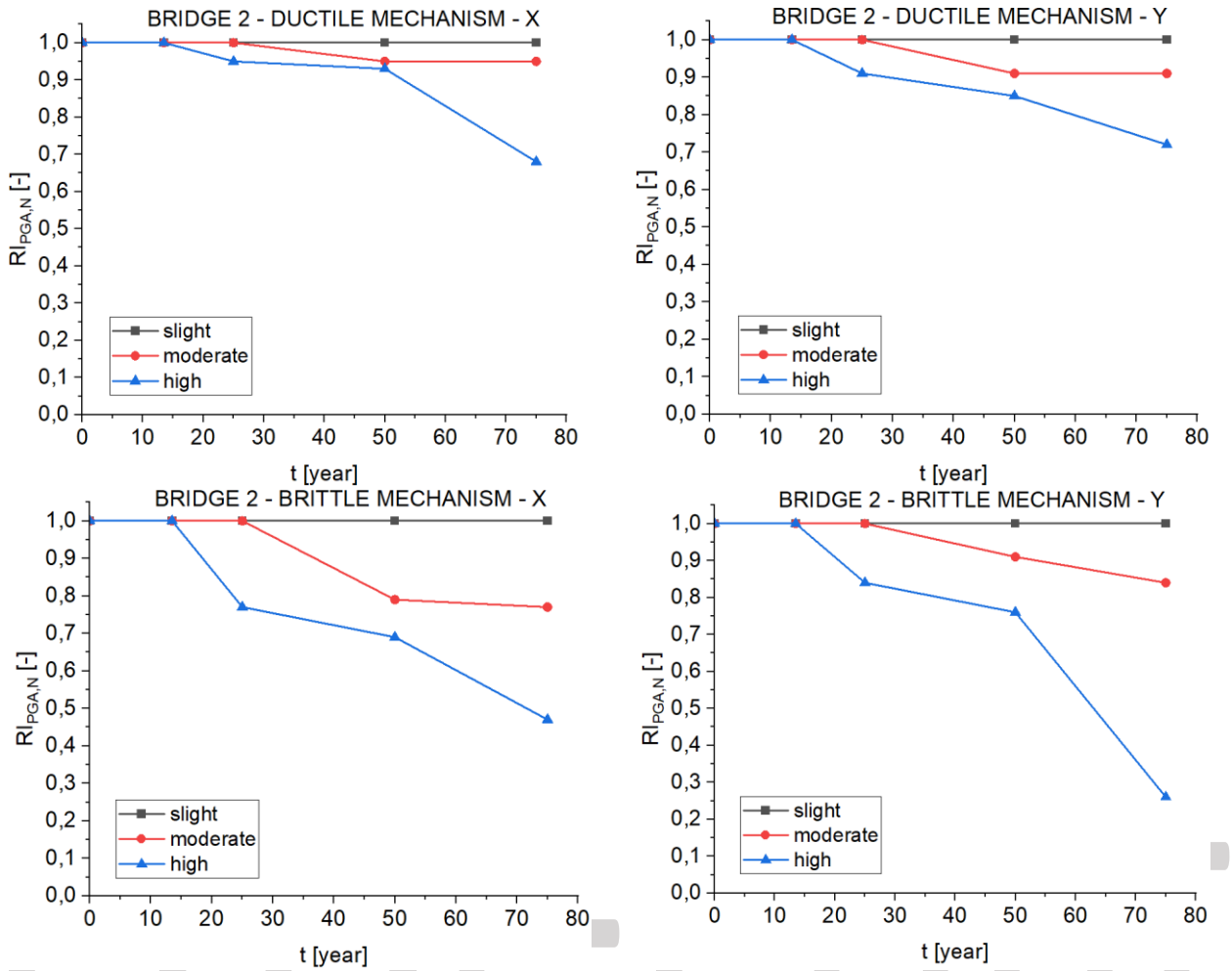


Figure 24. Evolution of the normalized PGA risk index, Bridge 2.

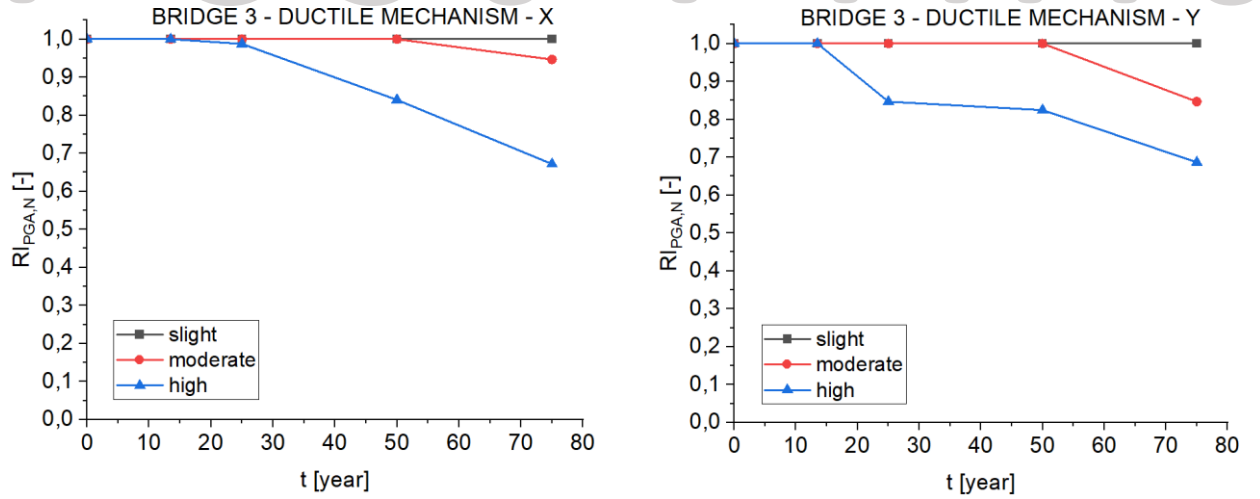

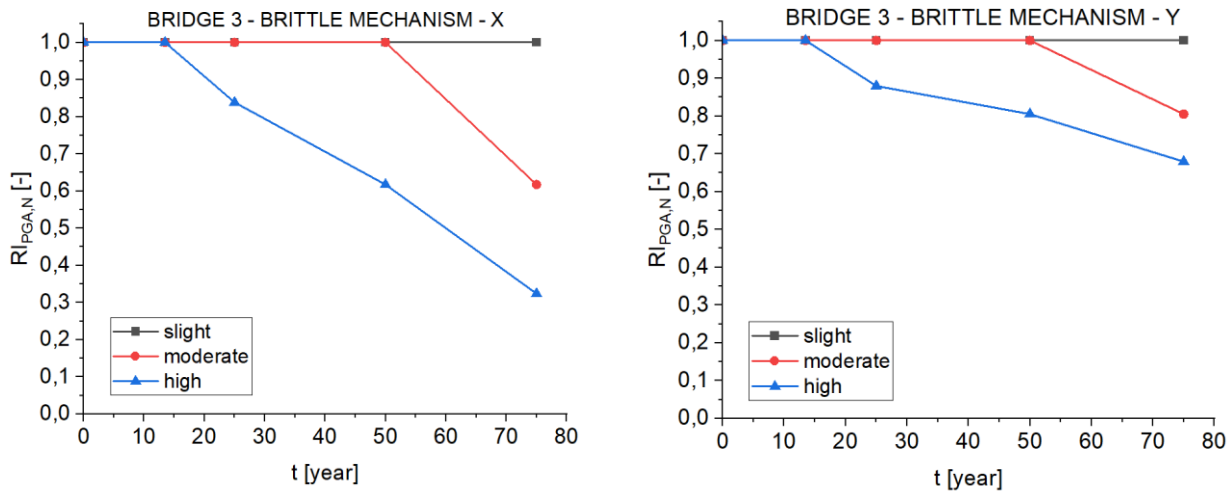


Figure 25. Evolution of the normalized PGA risk index, Bridge 3.

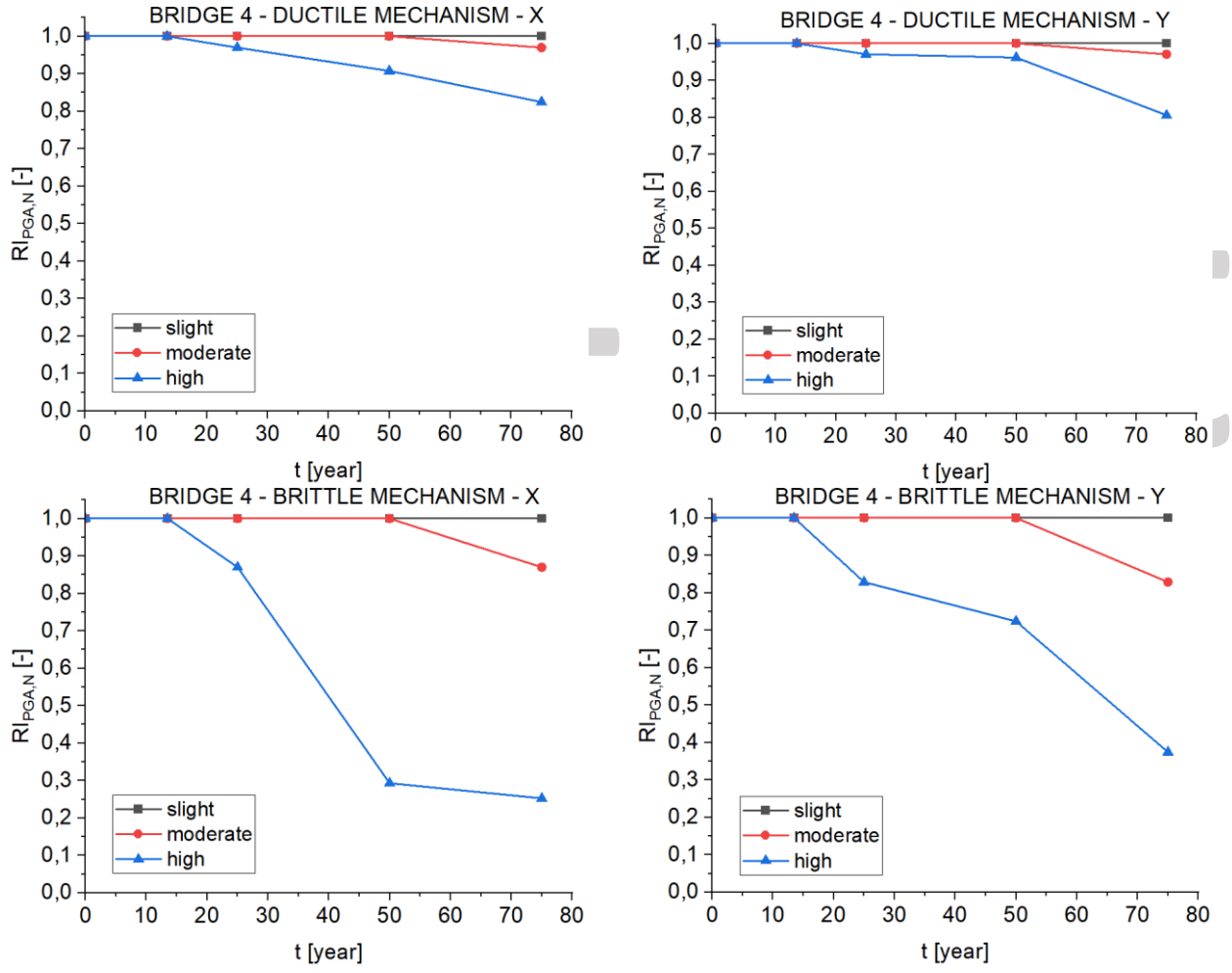


Figure 26. Evolution of the normalized PGA risk index, Bridge 4.

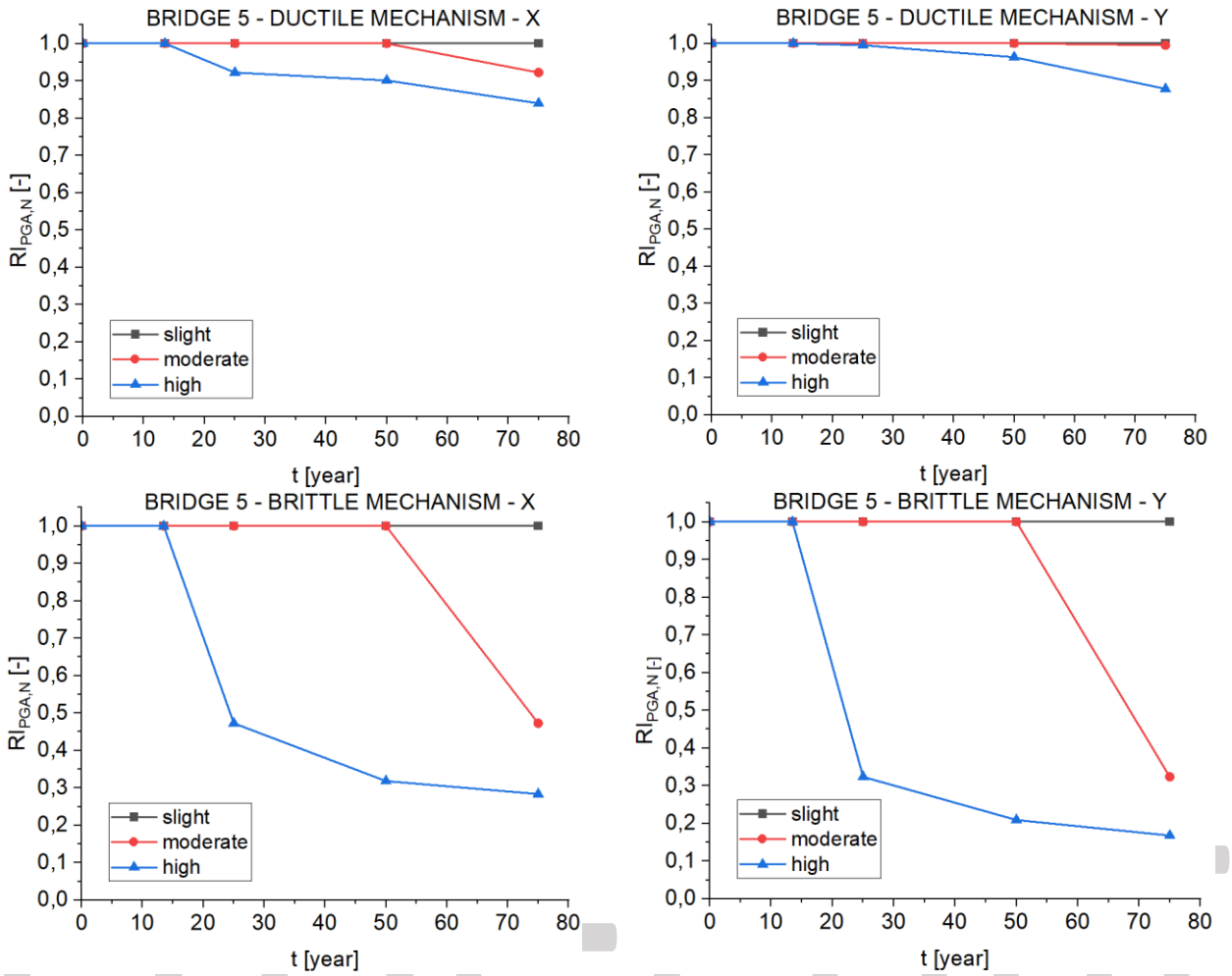


Figure 27. Evolution of the normalized PGA risk index, Bridge 5.

It is possible to notice that, as mentioned before, the value of the normalized PGA risk index significantly decreases for high corrosion levels, especially considering the brittle collapse mechanism, for all the bridges analysed. For moderate corrosion levels, always considering the brittle collapse mechanism, this reduction is evident only after 50 years since the construction of the bridges. According to the aforementioned results, slight corrosion levels do not significantly influence the seismic performance of the considered bridges.

## 4. Conclusions

In this paper, the seismic performance evolution over time of existing RC bridges subjected to corrosion effects induced by carbonation phenomenon is analysed. In particular, three different corrosion levels are here considered: slight, moderate, and high.

The seismic vulnerability is evaluated by means of a simplified procedure based on the implementation of finite element models of the bridges considering only beam elements and representing the non-linear behaviour of the structure through concentrated plastic hinges at the base of the piers. The foundations of the piers are modelled as fully constrained nodes at the base of each pier and consequently the soil-structure interaction effects are not considered. The corrosion effects due to carbonation phenomena are considered only in terms of steel reinforcement cross section reduction. A modal pushover approach was used and numerical analyses were performed on five existing RC bridges (built around 1960-1970 and located in moderate to high seismicity areas of Northern Italy) under three different corrosion scenarios, with the aim of obtaining the values of seismic risk indices considering both the ductile and brittle collapse mechanism of the piers.

The corrosion effects start after 13.5 years from the initial construction time of the RC bridges. Consequently, three fundamental time steps are considered: 25, 50, and 75 years after the construction time of the structures. By analysing the obtained results, it is possible to notice that the risk indices reduction is more evident for the brittle collapse mechanism that presents values lower than 1 even at the initial construction time of the bridges. This is due to the poor construction details mainly related to the transversal steel reinforcements of the Italian RC bridges built around 1960's.
Moreover, it is important to highlight that:

- the slight corrosion level does not lead to significant variations in terms of risk indices for all the above-mentioned time steps because of the low value of rebars cross area reduction that characterizes this corrosion scenario;
- after 25 years from the construction time of the bridges, the moderate corrosion scenario does not change the seismic performance of the structures. Furthermore, the high corrosion level shows significant reductions of the risk indices values, especially considering the brittle collapse mechanism that reaches values even equal to 82% (e.g. Bridge 5 in Y direction);
- after 50 years from the construction time of the bridges, the reduction of the risk indices values is significant even in case of moderate corrosion level, as it occurs for Bridge 5 in Y direction, where the reduction of the risk indices related to the brittle collapse mechanism exceeds 79%. Moreover, the high corrosion level always leads to important reductions of the risk indices considering the brittle failure mechanism for the case studies;
- after 75 years, both the moderate and high corrosion scenarios show significant reductions of the risk indices values even for the ductile collapse mechanism. The brittle mechanism reaches reductions greater than 50% in at least one of the two directions for all the analysed bridges.

The results obtained for the considered existing RC bridges show the importance of improving the maintenance and management of these kinds of structures through specific structural interventions and periodic assessment, by identifying the most critical structural members, which are characterized by the lowest risk index values and consequently impair the seismic performance of the considered structures.



## *References*


[1] Peng W, Tang Z, Wang D, Cao X, Dai F, Taciroglu E. A forensic investigation of the Xiaoshan ramp bridge collapse. Engineering Structures 2020; 224: 111203.

[2] Fan Y, Zhu J, Pei J, Li Z, Wu Y. Analysis for Yangmingtan bridge collapse. Engineering Failure Analysis 2015; 56: 20-27.

[3] Xu BX, Wang JT, Wang JX, Taciroglu E, Dai F, Peng W. A forensic investigation of the Taihe arch bridge collapse. Engineering Structures 2018; 176: 881-891.

[4] Sun J, Zhang J, Huang W, Zhu L, Liu Y, Yang J. Investigation and finite element simulation analysis on collapse accident of Heyuan Dongjiang Bridge. Engineering Failure Analysis 2020; 115: 104655.

[5] Birajdar HS, Maiti PR, Singh PK. Failure of Chauras bridge. Engineering Failure Analysis 2014; 45: 339-346.

[6] Tang L, Zhang EQ, Fu Y, Schouenborg B, Lindqvist JE. Concrete with hybrid functions – A novel approach to durable reinforced concrete structures. Materials and Corrosion 2012; 63(12): 1119-1126.

[7] Longarini N, Crespi P, Zucca M, Giordano N, Silvestro G. The advantages of fly ash use in concrete structures. Inzynieria Mineralna 2014; 15(2): 141-145.

[8] Zhang EQ, Abbas Z, Tang L. Predicting degradation of the anode–concrete interface for impressed current cathodic protection in concrete. Construction and Building Materials 2018; 185: 57-68.

[9] Van Nguyen C, Lambert P, Bui VN. Effect of locally sourced pozzolan on corrosion resistance of steel in reinforced concrete beams. International Journal of Civil Engineering 2020:1-12.

[10] Coni M, Mistretta F, Stochino F, Rombi J, Sassu M, Puppio ML. Fast falling weight deflectometer method for condition assessment of rc bridges. Applied Science 2021; 11(4): 1743.

[11] Zhou Y, Gencturk B, Willam K, Attar A. Carbonation-induced and chloride-induced corrosion in reinforced concrete structures. Journal of Materials in Civil Engineering 2014; 27(9): 1-17.

[12] Almusallan A. Effect of degree of corrosion on the properties of reinforcing steel bars. Construction and Building Materials 2001; 15: 361-368.

[13] Stefanoni M, Angst U, Elsener B. Corrosion rate of carbon steel in carbonated concrete – A critical review. Cement and Concrete Research 2018; 103: 35-48.

[14] Bertolini L, Elsener B, Pedeferri B, Polder R. Corrosion of steel in concrete. Prevention, diagnosis and repair. Wiley-VCH, Weinheim, 2004.

[15] Crespi P, Zucca M, Longarini N, Giordano N. Seismic assessment of six typologies of existing RC bridges. Infrastructures 2020; 5(6):52.

[16] Bossio A, Fabbrocino F, Monetta T, Lignola GP, Prota A, Manfredi G, Bellucci F. Corrosion effects on seismic capacity of reinforced concrete structures. Corrosion Reviews 2019; 37(1):45-56.

[17] Zhou H, Chen S, Du Y, Lin Z, Liang X, Liu J, Xing F. Field test of a reinforced concrete bridge under marine environmental corrosion. Engineering Failure Analysis 2020; 115: 104669.

[18] Pucci A, Puppio ML, Sousa HS, Geresini L, Matos JC, Sassu M. Detour-impact index method and traffic gathering algorithm for assessing alternative paths of disrupted roads. Transportation Research Record: Journal of Transportation research Board, August 2021.

[19] Valente M, Milani G. Alternative retrofitting strategies to prevent the failure of an under-designed RC frame. Engineering Failure Analysis 2018; 89: 271-285.

[20] Adhikari G, Pinho R. Development and application of Nonlinear Static Procedures for plan-asymmetric buildings. Research Report No. ROSE-2010/01. ROSE School, IUSS Pavia (Italy), 2010.

[21] Zucca M, Valente M. On the limitations of decoupled approach for seismic behaviour evaluation of shallow multi-propped underground structures embedded in granular soils. Engineering Structures 2020; 211: 110497.

[22] Zucca M, Crespi P, Longarini N. Seismic vulnerability assessment of an Italian historical masonry dry dock. Case Studies in Structural Engineering 2017; 7: 1-23.

[23] Zhang LW, Lu ZH, Chen C. Seismic fragility analysis of bridge piers using methods of moment. Soil Dynamics and Earthquake Engineering 2020; 134: 106150.

[24] Moridani KK, Zarfam P, Ashtiany MG. A novel and efficient hybrid method to develop the fragility curves of horizontally curved bridges. KSCE Journal of Civil Engineering 2020; 24: 508-524.

[25] Stefanidou S, Kappos A. Methodology for the development of bridge-specific fragility curves. Earthquake Engineering and Structural Dynamics 2017; 46(1): 73-93.

[26] Vamvatsikos D, Cornell AC. Incremental dynamic analysis. Earthquake Engineering and Structural Dynamics 2002; 31(3): 491-514.

[27] Bernuzzi C, Rodigari D, Simoncelli M. Incremental dynamic analysis for assessing the seismic performance of moment resisting steel frames. Ingegneria Simica 2020; 4.

[28] Paraskeva TS, Kappos AJ, Sextos AG. Extension of modal pushover analysis to seismic assessment of bridges. Earthquake Engineering and Structural Dynamics 2006; 35: 1269-1293.

[29] Paraskeva TS, Kappos AJ. Further development of a multimodal pushover procedure for seismic assessment of bridges. Earthquake Engineering and Structural Dynamics 2009; 39: 211-222.

[30] Chopra AK, Goel RK. A modal pushover procedure to estimate seismic demands of buildings. Earthquake Engineering and Structural Dynamics 2002; 31: 561-582.

[31] Chopra AK, Goel RK. A modal pushover analysis procedure to estimate seismic demands for unsymmetric-plan buildings. Earthquake Engineering and Structural Dynamics 2004; 33: 903-927.

[32] Crespi P, Zucca M, Valente M. On the collapse evaluation of existing RC bridges exposed to corrosion under horizontal loads. Engineering Failure Analysis 2020; 116: 104727.

[33] MIDAS Civil Analysis Reference, 2020.

[34] EN 1337-3:2005. Structural bearings – Part 3: Elastomeric bearings.

[35] EN 1998-3:2005. Eurocode 8: Design of structures for earthquake resistance – Part 3: Assessment and retrofitting of buildings. CEN (European Committee for Standardization), Management Centre. Brussels.

[36] Chen WF, Duan L. Bridge Engineering – Seismic Design, CRC Press, Boca Raton, FL, 2000.

[37] Miluccio G, Losanno D, Parisi F, Cosenza E. Traffic-load fragility models for prestressed concrete girder decks of existing Italian highway bridges. Engineering Structures 2021; 249: 113367.

[38] Decreto Ministeriale 17/01/2018, Ministero delle Infrastrutture e dei Trasporti, G.U. Serie Generale n.42 del 20/02/2018 – S.O.8.

[39] Kent DC, Park R. Flexural members with confined concrete. Journal of the Structural Division 1971; 97: 1969-1990.

[40] Park R, Paulay T. Reinforced Concrete Structures. John Wiley and Sons, New York, 1975.

[41] FEMA 356. Prestandard and commentary for the seismic rehabilitation of buildings. Federal Emergency Management Agency: Washington, DC.

[42] FEMA 440. Improvement of nonlinear static seismic analysis procedure. Applied Technology (ATC-55 Project) Department of Homeland Security, Federal Emergency Management Agency: Washington, DC.

[43] EN 1998-2:2005. Eurocode 8: Design of structures for earthquake resistance – Part 2: Bridges. CEN (European Committee for Standardization), Management Centre. Brussels.

[44] Saetta AV, Vitaliani R. Experimental investigation and numerical modeling of carbonation process in reinforced concrete structures: Part I: Theoretical formulation. Cement and Concrete Research 2004; 34(4): 571-579.

[45] Berto L, Vitaliani R, Saetta A, Simioni P. Seismic assessment of existing RC structures affected by degradation phenomena. Structural Safety 2009; 31: 284-297.

[46] Zanini MA, Pellegrino C, Morbin R, Modena C. Seismic vulnerability of bridges in transport networks subjected to environmental deterioration. Bulletin of Earthquake Engineering 2013; 11: 561-579.

[47] BRITE EURAM PROJECT BE 95-1347. Duracrete – probabilistic performance-based durability design of concrete structures.

[48] Bossio A, Monetta T, Bellucci F, Lignola GP, Prota A. Modeling of concrete cracking due to corrosion process of reinforcement bars. Cement and Concrete Research 2015; 71: 78-92.

[49] ATC-40:1996. Seismic Evaluation and Retrofitting of Concrete Buildings. Applied technology council, 8.1-8.66, Redwood City, CA, 1996.

[50] Causevic M, Mitrovic S. Comparison between non-linear dynamic and static seismic analysis of structures according to European and US provisions. Bulletin of Earthquake Engineering 2011; 9(2): 467-489.

[51] Fajfar P, Gaspersic P. The N2 method for the seismic damage analysis of RC buildings. Earthquake Engineering and Structural Dynamics 1996; 23: 23-67.

[52] Chopra AK. Dynamics of structures - theory and applications to earthquake engineering. 2nd edn., Prentice Hall, New Jersey, 2001.

[53] Stochino F, Fadda ML, Mistretta F. Assessment of RC Bridges integrity by means of low-cost investigations. Frattura ed Integrità Strutturale 2018; 46: 216-225.

[54] Sassu M, Geresini L, Puppio ML. Failure scenarios of small bridges in case of extreme rainstorms. Sustainable and Resilient Infrastructure 2017; 2(3): 108-116.

[55] Zucca M. Crespi P, Pasqualato G. On the seismic vulnerability evaluation of RC bridges exposed to corrosion. IABSE Congress, Christchurch 2020: Resilient Technologies for Sustainable Infrastructure, Proceedings, Christchurch, 3-5 February 2021: 471-478.